ELECTROCHEMISTRY OF DNA-MODIFIED SURFACES AND SENSING APPLICATIONS

by

Navanita Sarma
B. Sc., Gauhati University, India, 2000
M. Sc., Indian Institute of Technology, Guwahati, 2002

THESIS SUBMITTED IN PARTIAL FULFUILLMENT OF
THE REQUIREMENTS FOR THE DEGREE OF

MASTER OF SCIENCE

In the Department of Chemistry

SIMON FRASER UNIVERSITY

Fall 2006

APPROVAL

Name: Navanita Sarma

Degree: Master of Science

Title of Thesis: Electrochemistry of DNA - Modified Surfaces and Sensing Applications

Examining Committee:

Chair: Dr. George R. Agnes (Professor)

Dr. Hua-Zhong Yu (Associate Professor)
Senior Supervisor

Dr. Dipankar Sen (Professor)
Committee Member

Dr. Gary W. Leach (Associate Professor)
Committee Member

Dr. Melanie A. O'Neill (Assistant Professor)
Committee Member

Dr. Michael H. Eikerling (Assistant Professor)
Internal Examiner

Date Approved: November 9, 2006

ABSTRACT

The research objective of this thesis was to develop aptamer (nucleic acid receptor) -based electrochemical sensors for molecular analytes that are of biomedical importance. Three different experimental approaches for the characterization of DNA-modified surfaces have been explored. First, cyclic voltammetric (CV) responses of redox cations, such as $[Ru(NH_3)_6]^{3+}$, were analyzed to monitor the binding of lysozyme to aptamer-modified gold electrodes. It has been found that the decrease in the integrated charge of the electrostatically bound $[Ru(NH_3)_6]^{3+}$ is proportional to the analyte concentration. The second part of the thesis briefly describes the application of an intercalator, 9,10-anthraquinone-2,6-disulfonic acid, as an alternative redox label for studying DNA-modified surfaces. The last part describes the synthesis and characterization of ferrocene tethered oligonucleotides (Fc-DNA). The electrochemical behavior of gold electrodes modified with Fc-DNA-strands has been evaluated.

To my parents

ACKNOWLEDGEMENTS

I would like to sincerely thank my senior supervisor, Dr. Hua-Zhong (Hogan) Yu for giving me the opportunity to do research in his lab. I thank him for his guidance, encouragement and advice throughout my studies at SFU.

I express my sincere gratitude to Dr. Bixia Ge for her help during the past year. I thank her for all the discussions and helpful ideas.

I would like to thank my committee members, Dr. Gary Leach, Dr. Melanie O'Neill and Dr. Dipankar Sen for discussion and helpful suggestions. I would also like to thank Dr Michael Eikerling for agreeing to be my internal examiner. I thank Dr. Eberhard Kiehlman for proofreading my thesis.

I would like to thank the following people for their contribution during my graduate studies at SFU: Carlo Sankar and Li Su, for training me at the early stages of my project; Dr. Janet Huang and Edward Leung for training me in radioisotope labeling.

I thank all the past and present members of the Yu-Lab (Alan, Lily, Dr. Wang, Andy, Emily, Cassie, Dinah, Marcus, Hideh, Joe, Yunchao, Mandy, and Madhvi) for their friendship and making my stay at SFU worthwhile.

Last but definitely not the least I thank my parents and sisters, and my friend Salim for their constant support and encouragement.

TABLE OF CONTENTS

LIST OF FIGURES

LIST OF TABLES

LIST OF ABBREVIATIONS

AQ	Anthraquinone
AQDS	9, 10-Anthraquinone-2,6-disulfonic acid
A-T	Adenine and Thymine
ATP	Adenosine Triphosphate
C-G	Cytosine and Guanine
CV	Cyclic Voltammetry
DCC	Dicyclohexylcarbodiimide
DMT	Dimethoxytrityl
DNA	Deoxyribonucleic acid
ssDNA	Single-Stranded DNA
dsDNA	Double-Stranded DNA
NH_2-DNA	Ammine-terminated DNA
HS-DNA	Thiol-terminated DNA
Fc-DNA	Ferrocene-terminated DNA
DTT	Dithiotreitol
Γ_{DNA}	Surface Density of DNA
Fc	Ferrocene
FcA	Ferrocene Carboxylic Acid
Γ_{Ru}	Surface Concentration of $[Ru(NH_3)_6]^{3+}$
HPLC	High Performance Liquid Chromatography

LB	Leucomethylene Blue
MB	Methylene Blue
MCH	6-Mercapto-1-Hexanol
NHS	N-Hydroxysuccinimide
NMR	Nuclear Magnetic Resonance
Q	Integrated Charge
RNA	Ribonucleic acid
SAM	Self-Assembled Monolayer
SELEX	Systematic Evolution of Ligands by Exponential Enrichment
ssDNA/Au	Single-stranded DNA-modified gold electrodes
TCEP	Tris(2-carboxyethyl)phosphine hydrochloride
TEAA	Triethylammonium Acetate
THF	Tetrahydrofuran
Tris	Tris(hydroxymethyl)aminomethane

CHAPTER 1
GENERAL INTRODUCTION

As a general introduction to the background research for this thesis, the following sections will briefly describe the structure of DNA and aptamers, DNA surface chemistry, DNA biosensors and their applications, as well as previous achievements from our group and the objectives of the present work.

1.1 DNA and Aptamers

Deoxyribonucleic acid (DNA) is the cell's master repository of genetic information.[1a] The molecular principles behind gene technology, including DNA hybridization, amplification, and recombination, are all based on the double-helical structure of DNA molecules, which was first proposed by Watson and Crick in 1953.[2] This discovery was a turning point in the history of biological sciences, which opened up new opportunities for investigation of molecular details of gene structure and function. The complementary nature of the base pairing between the nitrogenous bases is the basis of replication of DNA double helices. DNA double helices are stabilized by both hydrogen bonding between the base pairs and base-stacking.

The structure of DNA consists of two polynucleotide strands that wind about a common axis with a right-handed twist to form an approximately 20 Å- diameter double helix.[1] The two strands are anti-parallel and wrap around each other such that they cannot

be separated without unwinding the helix. The bases occupy the core of the helix and the sugar-phosphate chains coil about its periphery, thereby minimizing the repulsions between charged phosphate groups. The planes of the bases are nearly perpendicular to the helix axis. Each base is hydrogen bonded to a base on the opposite strand to form a planar base pair. An ideal B-DNA helix has 10 base pairs (bp) per turn. Figure 1.1 shows a portion of double-stranded DNA (dsDNA) depicting how the bases, sugars and phosphate groups are connected.

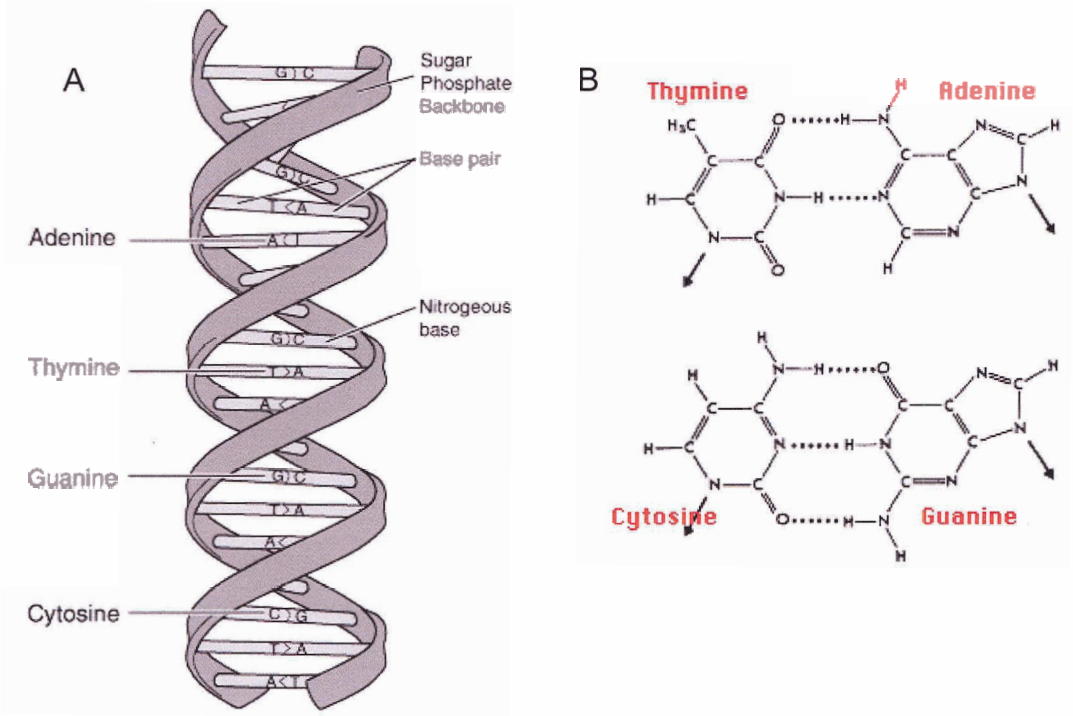

Figure 1-1 (A) Schematic representation of a portion of a DNA double helix showing the bonding between the bases, sugars and the phosphate groups. (B) Watson-Crick base-pairing between Adenine and Thymine, and Guanine and Cytosine respectively [Adapted from Ref. 1a]

The most remarkable feature of the Watson - Crick structure is that it generally accommodates two types of base pairs; each adenine residue must pair with a thymine residue and vice versa (A-T) and each guanine residue must pair with a cytosine and vice versa (G-C) (Figure 1B).

The right-handed B-DNA, as described above, is the biologically predominant but not the only form of DNA.[1a] When the relative humidity is reduced to 75%, B-DNA undergoes a reversible conformational change to the so-called A-DNA. A-DNA is also a right-handed helix, but it is shorter and wider than B-DNA. Compared to A-DNA and B-DNA, the Z-DNA is left-handed and can form alternating purine- pyrimidine tracts under certain conditions, including high salt concentration, the presence of certain divalent cations, or DNA supercoiling.[3]

Aside from being the molecule for the storage of genetic information, DNA offers a range of structural and physical properties that can be exploited *in vitro.* An aptamer is a DNA (or RNA) strand that is selected from large combinatorial libraries of oligonucleotides to bind to specific target molecules by *in vitro* selection or SELEX (systematic evolution of ligands by exponential enrichment).[4,5] The first aptamer (based on RNA) for small molecules was selected to target adenosine triphosphate (ATP), one of the most important cofactors in metabolism.[5a,b] Recently, aptamers made of single-stranded DNA (ssDNA) have been selected for many other small molecules, including organic dyes, porphyrins and arginine.[5b,c] Likewise, Huizenga and Szostak selected DNA aptamers for ATP and adenosine.[5d]

The advantages of aptamers over alternative approaches include the relatively simple techniques and apparatus required for their isolation, the number of alternative

molecules that can be screened and their chemical simplicity.[5e,f] Aptamers hold much promise as molecular recognition elements for incorporation into analytical devices, such as biosensors, affinity probe capillary electrophoresis, capillary chromatography, affinity chromatography and flow cytometry.

1.2 DNA Surface Chemistry

The essential role of a sensor is to facilitate the formation of the probe-target complex in such a way that the binding event can be easily reported.[6] Main components of a biosensor consist of a molecular recognition layer and a signal transducer that can be attached to a suitable electronic device (Figure 1-2).

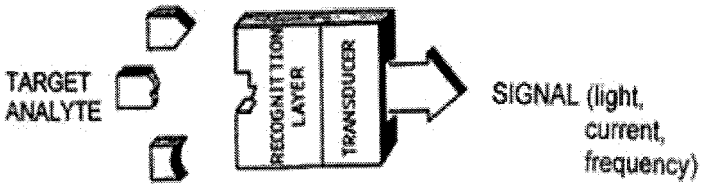

Figure 1-2 Main components of a biosensor: coupling of a recognition layer and a transducer. [Adapted with permission from Ref. 9]

DNA biosensors, based on nucleic acid recognition processes, are being developed towards the goal of rapid, simple and inexpensive testing of genetic and infectious diseases and for the detection of DNA damage and interactions.[7,8] Unlike

enzymes or antibodies, nucleic acid recognition layers can be easily synthesized and regenerated for multiple uses.[9]

Immobilization of DNA strands onto the transducer surface plays an important role in the overall performance of DNA biosensors.[9] Orientation of the probe molecules should be such that they are easily accessible for the target strands.[10] Depending on the nature of the transducer, there are various ways of immobilizing DNA probes onto the surface. These include the use of thiolated DNA for self-assembly onto gold surfaces; the use of biotinylated probes on avidin-coated gold surfaces; covalent (carbodiimide) coupling to hydroxyl groups on carbon electrodes; or a simple adsorption onto carbon surfaces.[9,11] Of particular interest is the immobilization of thiol-modified oligonucleotide (HS-DNA) probes on gold surface. Because of their simple preparation and characterization, they are among the most suitable for fundamental studies of DNA surface chemistry and potential applications in developing DNA-based biosensors.[9]

1.2.1 Thiolated DNA Monolayers on Gold and Their Characterization

Molecular self-assembly is one of the ubiquitous events in nature; it governs building of cell walls and folding of proteins.[12] In self-assembled monolayers (SAMs) formed on solid surfaces, the molecules display a higher degree of orientation, order and packing. SAMs of n-alkanethiols and their derivatives on gold are the most popular self-assembly systems that have been extensively studied.[13]

Similar to n-alkanethiols, thiol-modified oligonucleotides (HS-DNA) can be immobilized onto gold surfaces to form stable and closely packed monolayers.[14] One of the challenges is to control the surface density and orientation of DNA strands, which is critical for on-chip hybridization reactions.[15]

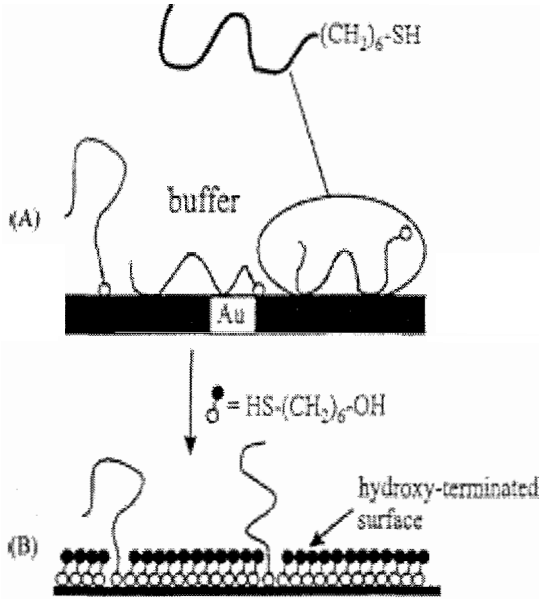

Figure 1-3 Schematic representation of preparation of a mixed thiol-modified single-stranded DNA/MCH monolayer. (A) adsorption of single-stranded DNA; (B) formation of mixed layer after adsorption of MCH. [Adapted with permission from Ref. 11]

Steel et al. have investigated the effect of DNA length and the presence of a thiol group on immobilization on gold surfaces.[14] They studied oligonucleotides with lengths from 8 to 48 bases, each containing a terminal 5'-hexanethiol anchoring group. It was shown that thiol groups strongly increase immobilization efficiency of oligonucleotide (i.e., a high surface density can be achieved), but this increase is reduced for longer strands. For oligonucleotides longer than 24 bases, the surface coverage begins to decrease which is consistent to the less ordered structure (presumably reflecting increasing polymeric behavior). To improve the monolayer quality, the DNA-modified surfaces were treated with a "blocking" reagent, 6-mecapto-1-hexanol (MCH), as shown

in Figure 1.3. The thiol group of MCH replaces weaker adsorptive contacts between DNA nucleotides and the gold substrates, leaving the probes tethered primarily through the thiol groups. After MCH-treatment, ssDNA swells and extends further into solution, thereby becoming highly accessible to the target strands.[6b]

Various techniques have been used to characterize DNA monolayers on gold, including scanning tunneling microscopy (STM), neutron reflectivity, X-ray photoelectron spectroscopy (XPS), ellipsometry, ^{32}P-radiolabeling, fluorescence labeling, surface plasmon resonance spectroscopy, and Fourier transform infra-red spectroscopy (FTIR).[16] Rekesh et al. have reported STM images of oligonucleotides on gold surfaces; ssDNA appeared as "blobs" while dsDNA appeared as "rodlike".[16a] Neutron reflectivity studies have shown that ssDNA pass from a compact configuration, suggesting the presence of multiple contacts between the DNA strands and the surface, to an extended configuration following the MCH treatment.[16b] Tarlov and co-workers suggested from XPS data that the strong thiol-gold interaction can drive the adsorption of thiolated DNA to a higher surface coverage, although they are not oriented perpendicular to the surface.[16c] They also used FTIR to determine the DNA surface coverage and DNA film structure.[16d]

1.2.2 Spectroscopic Study of DNA Modified Surfaces and Optical DNA Biosensors

Spectroscopic study of DNA-modified surfaces and detection of DNA-hybridization have gained considerable attention in the past.[17-20] Optical biosensors based on fluorescence are very sensitive, with detection limits approaching 10^7 molecules / cm^2.[20] They normally rely on fiber optic to transduce the emission signal of a fluorescent label. The operation typically involves placement of an ssDNA probe at the end of the

fiber and monitoring the fluorescence changes resulting from the association of a fluorescent indicator with the dsDNA hybrid. Another type of DNA-based optical biosensors, developed by Krull's group, relied on the use of an ethidium bromide indicator.[17a] Walt's group developed a sensor array for the simultaneous detection of multiple sequences by observing the increase in fluorescence upon binding of the complementary DNA. [17b]

Another type of optical transduction devices that offers real-time label-free detection of DNA hybridization is monitoring changes in surface optical properties resulting from the binding reaction.[18] Such devices combine the simplicity of surface plasmon resonance with the sensitivity of wave guiding devices. DNA optical sensors have been also developed based on the combination of sandwich solution hybridization, magnetic bead capture, flow injection and chemiluminescence for rapid detection of DNA hybridization.[19] For example, *in situ,* label-free, optical detection can be achieved using a novel nanoparticle-based colorimetric detection of DNA hybridization: a distance change between the nanoparticles due to the hybridization event results in changes of optical properties of the aggregated functional gold nanoparticles.[20] Another approach is based on the use of molecular beacons (oligonucleotides with a stem and loop structure), labeled with a fluorophore and a quencher at the two ends of the stem, that become fluorescent upon hybridization with the complementary strand.[21]

1.2.3 Electrochemical Study of DNA Modified Surfaces

Although the aforementioned spectroscopic methods are very popular and offer great sensitivity, the instruments are generally complex and expensive. Electrochemical methods offer an alternative approach for DNA diagnostics. High sensitivity coupled

with modern micro-fabrication technologies, portability, low cost, minimal power requirements and independence of sample turbidity or optical pathway make electrochemical transduction devices ideal candidates for DNA diagnostics.

The earliest electrochemical sensing scheme was based on reduction and oxidation of DNA at a mercury electrode; the amount of DNA reduced or oxidized reflects the amount of DNA adsorbed. More than 40 years ago, Palaćek and co-workers explored the use of electrochemical methods to differentiate between single-stranded and double-stranded DNA through direct oxidation/reduction of DNA on mercury electrode surfaces.[22]

Among the four DNA bases, guanine is most easily oxidized and this process has been studied on carbon, gold, indium tin oxide (ITO) and polymer-coated electrodes.[11,6] Adsorption stripping voltammetry (ASV) was the most widely used method for signal detection. Although this method is very sensitive, its application has been limited due to high background currents at potentials required for direct DNA oxidation.[6] Thus, physical separation methods have been designed to remove sources of background.[23]

Wang and Kawde developed a method where, the guanine bases on the probe strand were substituted by inosine bases, which also bind to cytosine, but its oxidation signal is well separated from that of guanine.[23b] Hybridization was detected based on the guanine signals of the target strand.

Electrochemical mediators have been used to detect oxidation of target DNA. A greatly enhanced guanine signal, and hence hybridization response, can be obtained by using the electrocatalytic action of a redox mediator, $[Ru(bpy)_3]^{2+}$.[24] This involves the following catalytic cycle:

$$[Ru(bpy)_3]^{2+} \longrightarrow [Ru(bpy)_3]^{3+} + e^- \quad (1)$$

$$[Ru(bpy)_3]^{3+} + G \longrightarrow [Ru(bpy)_3]^{2+} + G^+ \quad (2)$$

The presence of a guanine-containing target nucleic acid creates a catalytic cycle that results in a large current output.

Mikkelsen's group pioneered the development of electrochemical sensors using electrostatically bound redox labels.[25] In their work, single-stranded DNA was immobilized onto a glassy carbon electrode via physical adsorption. After exposing the modified electrode to the target strands, redox indicators, $[Co(phen)_3]^{3+}$ were introduced. The redox marker has a greater affinity for double-stranded DNA, and therefore higher cathodic peaks were observed in the CV responses upon hybridization. Recently, Steel et al. have reported the use of multiply-charged cations, $[Ru(NH_3)_6]^{3+}$ as redox labels to signal DNA hybridization on gold electrodes modified with thiolated oligonucleotide probes.[26] The amount of the redox cations bound electrostatically to the DNA-backbone was determined by chronocoulometry. This method can be used to quantitate both the surface density of the probes and the hybridization efficiency with target samples.

Barton and co-workers have examined the use of redox-active intercalators to investigate the DNA-mediated charge transport.[27] The intercalator was not used in the assay to report the amount of DNA or whether it is double-stranded versus single-stranded. Instead, it was utilized to test whether the DNA base-pair stacking mediates charge transport from the electrode surface to the intercalator bound to the top of the film. In a typical assay, thiolated DNA duplexes are self-assembled onto gold surfaces and treated with redox-active intercalators, like methylene blue (MB) or daunomycin (DM).

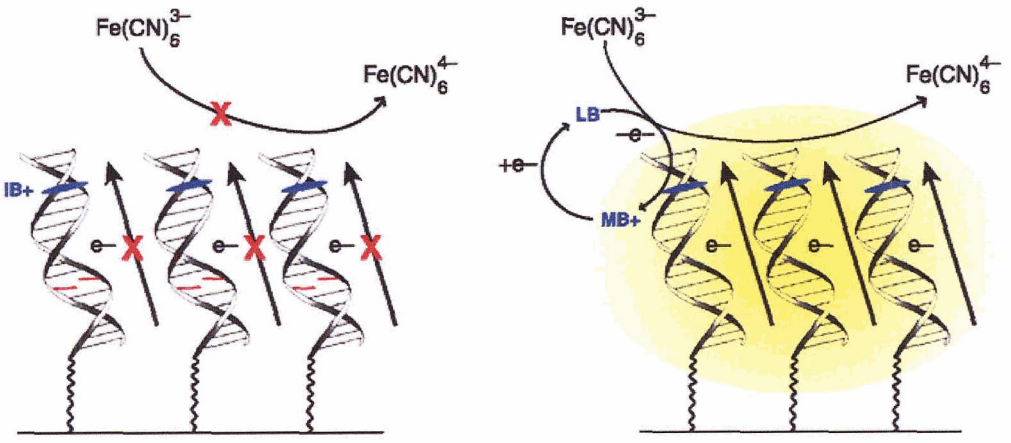

Figure 1-4 **Schematic representation of the electrocatalytic detection of DNA hybridization based on long-range electron transfer. [Adapted with permission from Ref. 6]**

It has been found that upon intercalation to the DNA double helix, the redox intercalator can either be reduced or oxidized via a DNA-mediated charge transport pathway. They further developed a catalytic strategy in which MB was used as a redox-label and ferricyanide as an electrocatalyst, to detect single-base pair mismatches.[27d] In this process, MB is reduced to leucomethylene blue (LB), and LB is then re-oxidized to MB by ferricyanide present in solution. The catalytic cycle continues as long as the potential on the electrode is sufficiently negative to reduce MB. The presence of a base mismatch decreases the electron transfer rate and the electrochemical response is noticeably reduced (Figure 1.4). Using this method, all of the possible single-base mismatches, including thermodynamically stable GA mismatches, can be detected. It has been demonstrated in their work that DNA-mediated charge transport may provide

specificity in mutation detection, sensitivity through electrocatalysis, and facile access to an array format.

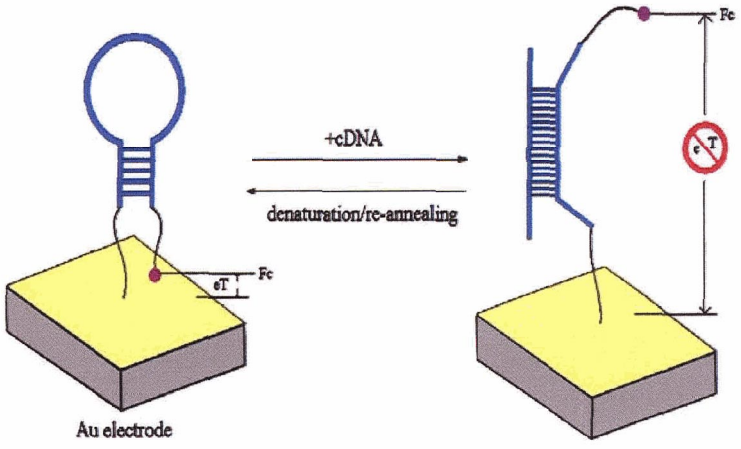

Figure 1-5 Schematic representation of the electrochemical DNA sensor attached to the gold electrode surface in the absence and presence of the target strand. [Adapted with permission from Ref. 29a]

Recently, several research groups have studied DNA-modified surfaces by covalently attaching a redox-active molecule (e.g., ferrocene) to one end of DNA through a short alkyl linker.[29] It is expected that hybridization with a complementary sequence changes the electrochemical response of the attached ferrocene moiety. For example, Heeger and co-workers used an electrode-attached, molecular beacon-like DNA stem-loop structure labeled with ferrocene as the hybridization sensing element.[29a] In the absence of the target DNA sequence, a pair of redox peaks is observed with the DNA-modified electrode; peak separation is consistent with a single-electron transfer reaction. Upon hybridization with the target sequence, a large decrease in the redox currents is observed. This can be explained as follows: in the absence of the target, the stem-loop structure holds the ferrocene tag into close proximity with the electrode surface, thus

ensuring rapid electron transfer and efficient redox of the ferrocene label (Figure 1.5). On hybridization with the target sequence, the ferrocene label is separated from the electrode surface and hence there is a decrease in the redox signal.

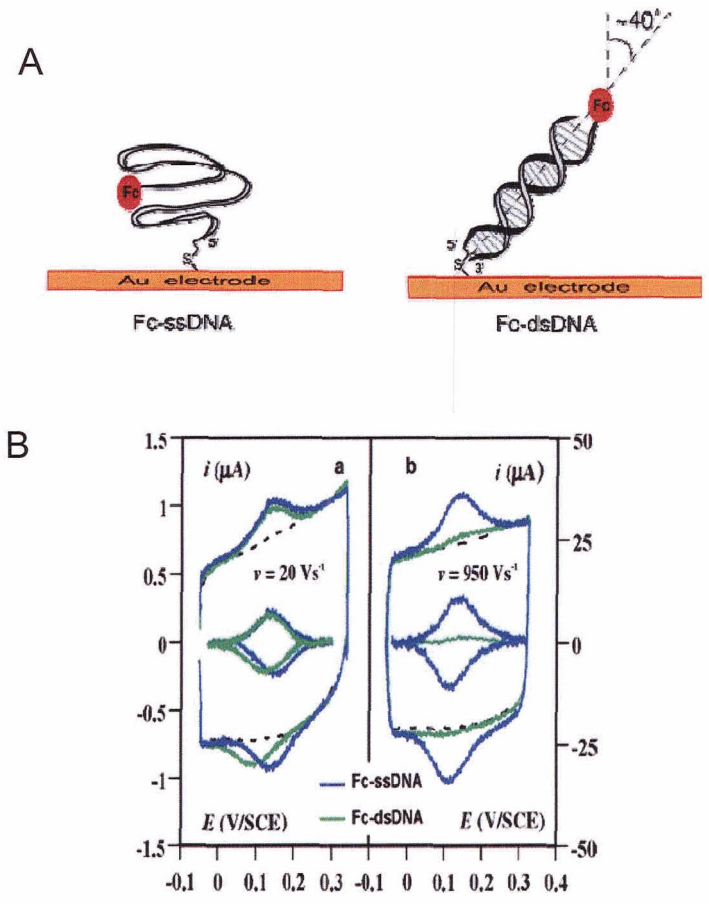

Figure 1-6 **(A) Scheme showing the alignment of Fc-labeled single-strand DNA and after hybridization with the non-labeled complementary strand. (B) The cyclic voltammograms for single-stranded and double-stranded DNA. The dashed curves correspond to the background signals, the blue curve is for single-stranded DNA and the green curve is for the double-stranded DNA. [Adapted with permission from Ref. 29c]**

Long et al. investigated the cross-strand electron-transfer properties in DNA duplex using a ferrocene-terminated DNA.[29b] Anne and co-workers studied the

relationship between the structure and electron transfer kinetics in DNA monolayers by covalently attaching a ferrocene moiety to the free DNA-terminus (Figure 1.5).[29c,d] Specific hybridization of the grafted-ssDNA chains with unlabeled complementary target in solution induce an unprecedented perturbation of the electrochemical response of the ferrocene heads that ultimately provide quantitative information on the deformability of a short tethered dsDNA. In their protocol, the ferrocene (Fc) moiety is attached to the 3'-end of the 20-mer DNA sequence, while the 5'-end of the same strand is grafted to a gold electrode (Figure 1.6A).

They observed that at low scan rates ($v \leq 20$ V/s), the voltammograms for the Fc-dsDNA modified surface are symmetric. The anodic and cathodic peak currents are proportional to the scan rate, and, the peak separation is small, indicative of a surface-confined species exhibiting an ideal Nernstian behavior. This behavior is similar as that of Fc-ssDNA modified surface, which ascertains that all the ferrocene heads are allowed to reach the electrode surface within the time-frame of the voltammogram and undergo reversible heterogenous electron-transfer reactions. However, at higher scan rates (v = 950 V/s), the voltammograms for ssDNA and dsDNA are different (Figure 1.6B). The voltammograms obtained for the double-stranded DNA is almost the same as the background signal, showing that the ferrocene groups cannot reach the electrode in the time-frame of the voltammogram and hence redox behavior is seen to decrease significantly.

1.3 Previous Work and Objectives of This Thesis

1.3.1 Electrochemical Procedure for the Investigation of DNA-Modified Surfaces

Previous publications from our laboratory have described a simple electrochemical procedure for analyzing DNA-modified surfaces, i.e., to quantify the density of DNA probes on the surface and to detect the on-chip hybridization of target strands from solution.[30] This protocol is based on the voltammetric responses of redox cations bound electrostatically to the DNA molecules on the surface. The success of this approach lies in the easy distinction of the surface redox peaks from the signals of the diffusion species using micromolar concentrations (μM). Compared to other electrochemical methods, the attractive feature of this method is the simplicity and ease of data interpretation. [31, 32]

The voltammetric protocol has been extended to explore the kinetics of metal ion-DNA interactions on surfaces and the study of non-electroactive cation-DNA interactions.[30b-c] The experiment involves the incubation of DNA-modified electrodes in a solution containing multiply charged transition metal complexes, such as $[Ru(NH_3)_6]^{3+}$, at low ionic strength. An ion-exchange equilibrium is readily established between these transition metal cations and the native charge compensation ions associated with the negative DNA backbone.[26, 30a] A schematic representation of this event and the corresponding cyclic voltammograms is shown in Figure 1.7.

The surface concentration of $[Ru(NH_3)_6]^{3+}$, Γ_{Ru} (mol/cm^2) can be calculated using the following equation:

$$\Gamma_{Ru} = \frac{Q}{nFA} \qquad 1.1$$

where Q is the charge obtained by integrating the reduction peak area of surface-bound $[Ru(NH_3)_6]^{3+}$, n is the number of electrons involved in the redox reaction, F is the Faraday constant and A is the electrode area. The peak area for integration is obtained by subtracting the background (i.e., the capacitive current) from the voltammetric signals of the $[Ru(NH_3)_6]^{3+}$, as shown in Figure 1.8.

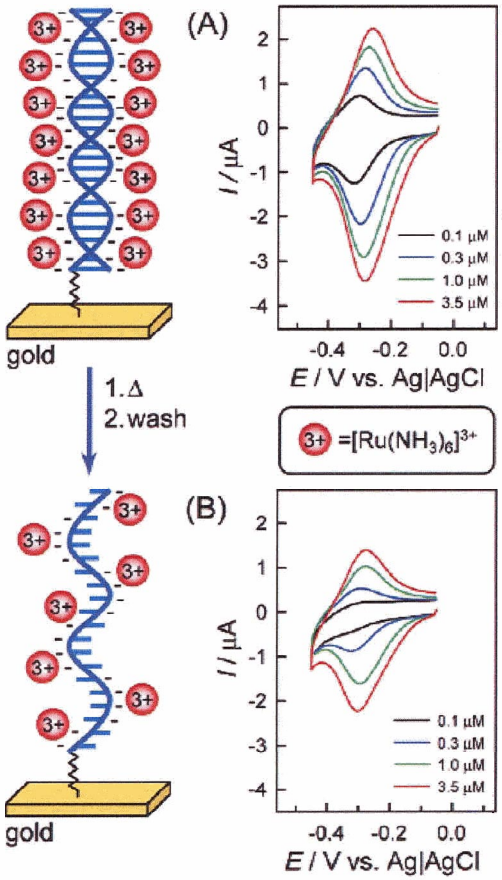

Figure 1-7 **Schematic representation and voltammetric responses of multiply-charged transition metal cations bound electrostatically to the DNA-modified surfaces: cyclic voltammograms of gold electrodes modified with (A) double-stranded DNA and (B) single-stranded DNA. The scan rate was 50 mV/s. [Adapted with permission from Ref. 30a]**

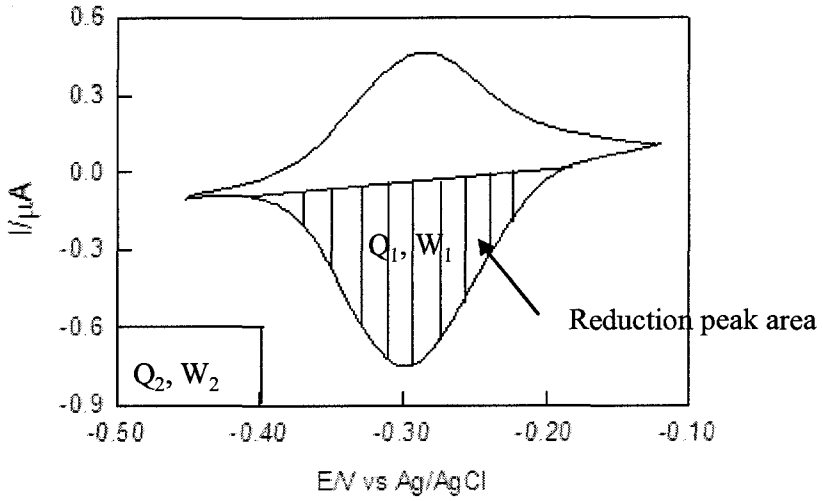

Figure 1-8 Cyclic Voltammograms of dsDNA-modified electrode in 10 mM Tris buffer in the presence of 5.0 μM $[Ru(NH_3)_6]^{3+}$. The scan rate is 0.1V/s.

Integration for the reduction peak area of $[Ru(NH_3)_6]^{3+}$ is usually done by the μAutolab GPES software. However, integration is difficult in cases where the peak area is very small. Under those circumstances, the following method has been used.

The traditional method of deriving the charge (Q_1) from the reduction peak area is done by cut-and-weigh method using the following equation:

$$Q_1 = \frac{W_1}{W_2} Q_2 \qquad 1.2$$

where W_1 and W_2 are the weight of the paper corresponding to the area under the reduction peak (the shaded area in Figure 1.8) and a known area (the boxed region in Figure 1.8) and respectively. Q_2 is the charge calculated from the boxed region using the following equation:

$$Q_2 = E\frac{I}{\nu} \qquad 1.3$$

Where, I and E are the current and potential derived directly from the x- and y-axis, respectively; ν is the scan rate used for the measurement. The calculated value of Q_1 can be used in equation 1.1 to calculate the surface density of $[Ru(NH_3)_6]^{3+}$ on the electrode.

Under saturation conditions (based on the adsorption isotherm), the measured value of Γ_{Ru} can be converted to the surface density of DNA, Γ_{DNA}, using the following relationship:

$$\Gamma_{DNA} = \Gamma_{Ru}(\frac{z}{m})N_A \qquad 1.4$$

where *z* is the charge of the redox cation, *m* is the number of nucleotides in the DNA. The maximum surface density of double-stranded DNA estimated theoretically is (5.2×10^{12} molecules/cm^2), assuming a compact DNA monolayer on the electrode surface and that the double-helices "stand" on the surface with a small tilt angle relative to the normal.[30a]

1.3.2 Design of Deoxyribosenors for Specific Detection of Molecular Analytes

The dependence of the conductivity of DNA on its conformational state has been exploited for the fabrication of electronic biosensors. Dr. Sen's group has shown that the binding of ligand can change the conformation of the aptamer, leading to electrical conduction through the DNA double helix (Figure 1.7).[33a]

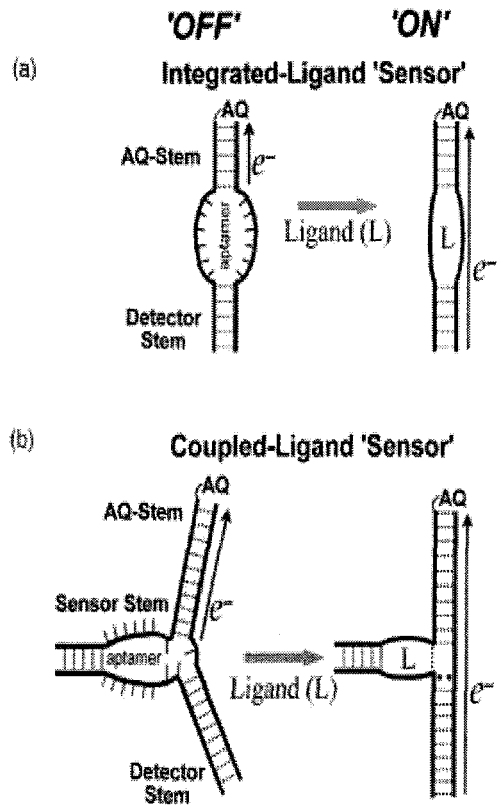

Figure 1-9 **Design of the (a) "integrated-ligand" and (b) "coupled-ligand" aptamer sensor. In the absence of the analyte the sensor has an open, unstructured conformation, which only permits electron transfer in the AQ-stem. However, analyte-binding changes the conformation of the sensor to a more compact form, thereby leading to electron-transfer through the entire DNA helix. [Adapted with permission from Ref. 33b]**

Adenosine is an uncharged compound incorporating a heterocyclic base, and it is an essential component of nucleic acids. The adenosine aptamer sequence has been "discovered" by Huizenga and Szostak.[34] High resolution NMR studies on this aptamer have shown a typical adaptive folding, i.e., it forms a hydrogen-bonded and stacked helical structure upon adenosine binding.[35]One aptamer binds two adenosine molecules,

and upon binding to adenosine the aptamer's loose structure compacts to a tightly hydrogen-bonded, base-stacked helical structure.

Two different types of "dexoyribosensors" have been proposed by Dr. Sen's groups: the "integrated-ligand" sensor that incorporates the receptor (aptamer) into its conduction path, while the "coupled-ligand" sensor places its receptor adjacent to a distorted conduction path; both paths are rectified upon ligand binding. Charge-transfer in these constructs is initiated by photoexcitation of an anthraquinone (AQ) moiety attached through a $-(CH_2)_6-$ linker to the AQ stem of each construct. When tested for detection of charge flow, both sensor designs gave higher levels of charge conduction in their detection stems in response to adenosine binding.

This idea of charge conduction through DNA double helices was later extended to design other coupled-ligand aptamer sensors for diverse analytes. Another "coupled-ligand" sensor was designed for L-arginamide, a non-heterocyclic analyte with a positive charge.[33b] This DNA aptamer was developed by Harada and Frankel, with a dissociation constant of 100 μM for L-arginamide.[36] It was shown by Dr. Sen's group that specific binding of this ligand also promotes charge conduction through the detector stem of the sensor construct due to the change in conformation.[33b] This research shows that deoxyribosensors have potential applications for sensing biological macromolecules, including proteins and other nucleic acids.

1.3.3 Objectives of This Thesis

This thesis explores the application of simple electrochemical methods in sensing aptamer-ligand (analyte) interactions, particularly analyte molecules that are of biomedical importance. As mentioned previously, DNA (aptamer) can be labeled with

redox-active probes in three different ways: covalent binding, electrostatic interaction, and intercalation. We intended to explore and compare these three different methods.

All the three methods have their own advantages and disadvantages. Covalent binding of redox center to DNA strands provides direct electrochemical signal that is corresponding to the quantity of DNA probes/targets on surfaces, but does involve tedious synthesis and purification steps. Intercalative and electrostatic binding of redox labels are easier to prepare, but rely on the assumption that adsorption equilibrium is achieved. In many cases, the quantitation is not straightforward either. In this thesis, we will first focus on the application of electrostatic method to investigate apatmer-ligand interactions, and then will also provide some preliminary results on the other two approaches.

Specifically, Chapter 2 will study the detection of protein (lysozyme) binding to aptamer-modified gold electrodes by monitoring the cyclic voltammetric response of multiply-charged redox cations, such as $[Ru(NH_3)_6]^{3+}$, which electrostatically interact with the DNA (aptamer) backbones. The selectivity of the aptamer for lysozyme and specificity of this electrochemical sensor will be investigated. Chapter 3 will illustrate the feasibility of using DNA intercalators, e.g., 2,6-anthraquinone-9,10-disulfonic acid (AQDS) as an alternative redox-active indicator in the electrochemical sensor application. Chapter 4 explores the synthesis of an oligonucleotide terminated with a redox-marker, ferrocene (Fc-DNA) and the electrochemical behavior of (Fc-DNA)-modified gold electrode.

1.4 References

1. Voet, D. and Voet, J.; *Biochemistry* 3rd Edition, John Wiley and Sons, **2004.**
2. Watson, J. D.; Crick, F. H. C. *Nature* **1953**, *171*, 737-738.
3. Sinden, R. R.; *DNA Structure and Function,* Academic Press, San Diego, **1994,** pp 25-31.
4. (a) Tuerk, G.; Gold, L. *Science* **1990,** *249*, 505-510; (b) Ellington, A. D.; Szostak, J. W. *Nature* **1990,** *346,* 818-822.
5. For example see: (a) Sassanfar, M.; Szostak, J. W. *Nature* **1993**, *364*, 550-553; (b) *Aptamer Handbook,* Wiley- VCH, Weinheim, **2006**; (c) Wilson, D. S.; Szostak, J. W. *Annu. Rev. Biochem.* **1999,** *68, 611-647*; (d) Huizenga, D. E.; Szostak, J. W. *Biochemistry* **1995**, *34*, 656-665; (e) Jayasena, S. *Clin. Chem.* **1999**, *45*, 1628-1650; (f) *Molecular Analysis and Genome Discovery,* Chichester, England; Hoboken, N.J.; J. Wiley, **2004**; 191-209;
6. Drummond, T. G.; Hill, M. G.; Barton, J. K. *Nat. Biotechnol.* **2003**, *21*, 1192-1199.
7. Christopoulos, T. K. *Anal. Chem.* **1999**, *71*, 425R-438R;
8. Palacek, E.; Fojta, M.; Tomschick, M.; Wang, J. *Biosens. Bioelectron.* **1998**, *13*, 621-628
9. Wang, J. *Nucleic Acids Res.* **2000**, *28*, 3011-3016.
10. (a) Herne, T. M.; Tarlov, M. J. *J. Am. Chem. Soc.* **1997**, *119*, 8916-8920. (b) Kelley, S. O.; Jackson, N. M.; Hill, M. G.; Barton, J. K. *Angew. Chem. Int. Ed.* **1999**, *38*, 941-945. (c) Hartwich, G.; Caruana, D. J.; de Lumley-Woodyear, T.; Wu, Y. B.; Campbell, C. N.; Heller, A. *J. Am. Chem. Soc.* **1999**, *121*, 10803-10812.
11. Wang, J. *Analytica chimica Acta,* **2002**, *469*, 63-71.
12. Poirier, G. E. *Langmuir,* **1999**, *15*, 1167-1175.

13. (a) Ulman, A. *Characterization of Organic Thin Films* **1995;** pp 24-27. (b) Ulman, A. *An Introduction to Ultrathin Organic Films: from Langmuir-Blodgett to Self-Assembly*, Academic Press: San Diego, **1991**, pp 279-297.

14. Steel, A. B.; Levicky, R. L.; Herne, T. M.; Tarlov, M. J. *Biophy. J.* **2000**, *79*, 975-981.

15. Aqua, T.; Naaman, R.; Daube, S. S. *Langmuir* **2003**, *19*, 10573-10580.

16. (a) Rekesh, D.; Lyubchenko, Y.; Shlyakhtenko, L.; Lindsay, S. M.; *Biophys. J.* **1996**, *71*, 1079-1086; (b) Levicky, R.; Herne, T. M.; Tarlov, M. J.; Satija, S. K. *J. Am. Chem. Soc.* **1998**, *120*, 9787-9792; (c) Herne, T. M.; Tarlov, M. J. *J. Am. Chem. Soc.* **1997**, *119*, 8916-8920; (d) Petrovykh, D. Y.; Suda, H., K-S.; Whitman, L. J.; Tarlov, M., J. *J. Am. Chem. Soc.* **2003**, *125*, 5219-5226.

17. (a) Piunno, P.; Krull, U.; Hudson, R.; Damha, M.; Cohen, H. *Anal. Chem.,* **1995**, *67,* 2635-2643. (b) Ferguson, J. A.; Boles, T.; Adams, C.; Walt, D. *Nat. Biotechnol.* 1996, *14,* 1681-1684.

18. (a) Watts, H.; Yeung, D.; Parkesh, H. *Anal. Chem.,* **67,** *1995,* 4283-4289. (d) Thiel, A.; Frutus, A.; Jordan, C.; Corn, R.; Smith, L. *Anal. Chem.* **1997,** *69,* 4984-4956.

19. Chen, X.; Zhen, X.; Chai, Y.; Hu, W.; Zhang, Z.; Zhang, X.; Cass, A. E. *Biosens. Bioelectron.* **1998,** *13,* 451-458.

20. Storhoff, J.; Elghanian, R.; Mucic, C.; Mirkin, C.; Letsinger, R. *J. Am. Chem. Soc.* **1998,** *120,* 1959-1964.

21. Fang, X.; Liu, X.; Schuster, S.; Tan, W. *J. Am. Chem. Soc.* **1999,** *121,* 2921-2922.

22. Palaćek, E. *Nature* **1960**, *188*, 656-657.

23. (a) Jelen, F.; Yosypchuk, B.; Kourilova, A.; Novotny, L.; Palaćek, E.; *Anal chem.* **2002**, *74*, 4788-4793; (b) Wang, J.; Kawde, A. B. *Analyst* **2002**, *127*, 383-386.

24. (a) Johnston, D. H.; Glasgow, K. C.; Thorp, H. H. *J. Am. Chem. Soc*, **1995**, *117*, 8933-8938; (b) Yang, I. V.; Thorp, H. H. *Anal. Chem.* **2001**, *73*, 5316-5322.

25. (a) Millan, K. M.; Mikkelsen, S. R. *Anal. Chem.* **1993**, *65*, 2317-2323. (b) Millan, K. M.; Saraullo, A.; Mikkelsen, S. R. *Anal. Chem.* **1994**, *66*, 2943-2948.

26. Steel, A. B.; Herne, T. M.; Tarlov, M. J. *Anal. Chem.* **1998**, *70*, 4670-4677.

27. (a) Boon, E. M.; Barton, J. K. *Curr. Opin. Struc.l Biol.* **2002**, *12*, 320-329. (b) Kelley, S. O.; Barton, J. K.; Jackson, N. M.; Hill, M. J. *Bioconj. Chem*, **1997,** *8*, 31-37; (c) Boon, E. M.; Salas, J. E.; Barton, J. K. *Nat Biotechnol* **2000**, *18*, 1096-1100; (d) Kelley, S.O.; Boon, E. M.; Barton, J. K.; Jackson, N. M.; Hill, M, G. *Nucleic Acids Res.* **1999**, *27*, 4830-4837.

28. Gooding, J. *Electroanalysis* **2002,** *14,* 1149-1156.

29. (a) Fan, C.; Plaxco, K. W.; Heeger, A. J. *Proc. Natl. Acad. Sci. USA;* **2003**, *100*, 9134-9137 (b) Long, Y-T; Li, C-Z; Sutherland, T. C.; Chahma, M.; Lee, J. S.; Kraatz, H-B. *J. Am. Chem. Soc*, **2003**, *125,* 8724-25; (c) Anne, A.; Bouchardon, A.; Moiroux, J. *J. Am. Chem. Soc*, **2003**, *125*, 1112-1113; (c) Anne, A.; Demaille, C. *J. Am. Chem. Soc*, **2006**, *128*, 542-557.

30. (a) Yu, H-Z; Luo, C-Y; Sankar, C. G.; Sen, D. *Anal. Chem.* **2003**, *75*, 3902-3907; (b) Su, L.; Sankar, C. G.; Sen, D.; Yu, H-Z. *Anal. Chem.* **2004**, *76*, 5953-5959; (c) Su, L.; Sen, D.; Yu, H-Z. *Analyst* **2006**, *131*, 317-322.

31. (a) Yu, C. J.; Wan, Y. J.; Yowanto, H.; Li, J.; Tao, C. L.; James, M. D.; Tan, C. L.; Blackburn, G. F.; Meade, T. J. *J. Am. Chem. Soc.* **2001**, *123*, 11155-11161. (b) Kertesz, V.; Whittemore, N. A.; Chambers, J. Q.; McKinney, M. S.; Baker, D. C. *J. Electroanal. Chem.* **2000**, *493*, 28-36. (c) Whittemore, N. A.; Mullenix, A. N.; Inamati, G. B.; Manoharan, M.; Cook, P. D.; Tuinman, A. A.; Baker, D. C.; Chambers, J. Q. *Bioconjugate Chem.* **1999**, *10*, 261-270.

32. (a) Patolsky, F.; Weizmann, Y.; Willner, I. *J. Am. Chem. Soc.* **2002**, *124*, 770-772. (b) Patolsky, F.; Katz, E.; Willner, I. *Angew. Chem. Int. Ed.* **2002**, *41*, 3398-3402. (c) Gore, M. R.; Szalai, V. A.; Ropp, P. A.; Yang, I. V.; Silverman, J. S.; Thorp, H. H. *Anal. Chem.* **2003**, *75*, 6586-6592. (d) Kim, E.; Kim, K.; Yang, H.; Kim, Y. T.; Kwak, J. *Anal. Chem.* **2003**, *75*, 5665-5672.

33. (a) Fahlman, R.P; Sen, D. *J. Am. Chem. Soc.* **2002,** *124,* 4610-4616. (b) Sankar, C.G.; Sen, D. *J. Mol. Biol.* **2004,** *340,* 459-467.

34. Huizenga, D. E.; Szostak, J. W. *Biochemistry* **1995**, *34*, 656-665.

35. Lin, C. H; Patel, D. *J. Chem. Biol.* **1997**, *4,* 817-832.

36. Harada, K; Frankel, A.D. *Embo. J.* **1995,** *14*, 5798-811.

CHAPTER 2
APTAMER-BASED BIOSENSORS FOR LABEL-FREE VOLTAMMETRIC DETECTION OF LYSOZYME

An aptamer-based biosensor for the label-free voltammetric detection of lysozyme, a positively charged protein that plays a crucial role in the human body, has been developed. In particular, anti-lysozyme aptamer strands were immobilized on gold electrode surfaces via Au-S bonding. Upon incubation in $[Ru(NH_3)_6]^{3+}$ solutions, these modified electrodes respond to the presence of nanomolar concentration of lysozyme, which is indicated by the decrease of the reduction peak area of the surface-bound redox cations. The dependence of the sensor sensitivity on the surface-density of aptamer strands has also been investigated.

2.1 Introduction

Biosensors are devices for the detection of biological analytes, combining biological components with physicochemical detector systems. Due to the potential applications in clinical diagnosis and genome mutation detection, DNA-based biosensors are developed by immobilizing oligonucleotides on solid substrates.[1] A novel type of biosensors that has gained great attention these days is the aptamer-sensor.[2] As introduced in Chapter 1, aptamers, or nucleic acid receptors, are DNA or RNA molecules selected from a large random sequence pool and designed to bind to specific target

molecules.[3] Due to strong binding capability, ease of preparation and ability of interaction with a broad range of targets (metal ions, organic dyes and proteins), aptamer sensors are promising in the fields of biomedical analysis and diagnostics. Most aptamer-based sensors reported to date rely on conventional detection methods, such as fluorescence or nanoparticle tracers.[4,5]

Previous publications from our group have documented a simple electrochemical procedure to examine DNA-modified surfaces, i.e., quantitation of the surface density of DNA probes on the gold electrodes, investigation of cationic binding activity as well as electron-transfer kinetics.[6] In this chapter, we demonstrate that this method can be extended to the quantitative analysis of protein-DNA (aptamer) interactions. More specifically, the binding of lysozyme to aptamer-modified gold surface was investigated electrochemically. Lysozyme is a globular protein with 129 amino acids, molecular weight of 14 kDa and an isoelectric point (pI) of 11.[5] It is present in the mucosal membranes that line the human nasal cavity and tear ducts. Lysozyme is commonly referred to as the body's own antibiotic and plays a crucial role in the human body. An increase in concentration levels (at ~ 8 μg/ mL) causes immune system disorders.[7]

Anti-lysozyme aptamers were developed ("selected") by Ellington's group at the University of Texas, Austin.[8] The anti-lysozyme aptamers have dissociation constants (K_d) of 31 nM for lysozyme.[8,9] The same group has further developed a reusable, aptamer-based optical sensor for the detection and quantitation of protein binding.[10] For this purpose, the aptamer was immobilized on silica beads via streptavidin-biotin interaction and introduced into micro-machined chips on an electronic tongue sensor array. The Cy3-labeled lysozyme can be detected with a detection limit of 320 ng/mL.

Recently, Rodriguez et al. studied lysozyme binding to aptamer-modified indium-tin oxide (ITO) electrodes by electrochemical impedance spectroscopy, a relatively complex technique.[11] Nevertheless, they observed that with an increase in the concentration of lysozyme, the charge transfer resistance of $[Fe(CN)_6]^{3-}$ from the solution to the electrodes decreased. In the present work, we explore a simple, alternative electrochemical method for the detection of protein-aptamer binding based on the voltammetric response of multiply-charged transition metal cations, $[Ru(NH_3)_6]^{3+}$, bound electrostatically to the aptamer probes on the electrode surface.

2.2 Experimental Section

2.2.1 Materials

The synthetic oligonucleotide DMTO-$(CH_2)_6$-S-S-$(CH_2)_6$-O-5'-ATC TAC GAA TTC ATC AGG GCT AAA GAG TGC AGA GTT ACT TAG-3' was purchased from Core DNA Services Inc. (Calgary, AB). The 5'-thiol modifier was obtained from Glen Research (Sterling, VA). The design of the aptamer sequence is based on the sequences developed by Ellington's group for specific detection of lysozyme.[8, 10]

Glass slides coated with 5 nm chromium and 100 nm gold were obtained from Evaporated Metal Film (EMF) Inc. (Ithaca, NY). 6-Mercapto-1-hexanol (MCH), hexaammine ruthenium (III) chloride (98%), potassium ferricyanide (98%), 11-mercaptoundecanoic acid, lysozyme (95%) and Tween-20 were purchased from Sigma-Aldrich (Milaukee, WI) and used as received. Deionized water (>18.3 MΩ.cm) was from a Barnstead Easy Pure UV/UF compact water system (Dubuque, IA).

2.2.2 DNA Purification

The disulfide-modified oligomer was purified by reverse-phase HPLC on a Gemini 5-μm C18/110 Å column (Phenomenex, Torrance, CA), eluting with a gradient of 0.1 M triethylammonium acetate (TEAA) / CH_3CN (20:1) and CH_3CN at 1.0 mL/min. The sample was then treated with 10 mM TCEP (triscarboxyethylphosphine) in 100 mM Tris-buffer at pH 7.5 for 4 hours and desalted through a MicroSpin G-50 Column (G-50 Sephadex) to yield thiol-tethered single-stranded DNA (ssDNA), HS-$(CH_2)_6$-O-5'ATC TAC GAA TTC ATC AGG GCT AAA GAG TGC AGA GTT ACT TAG-3'. The purified sample was then heated to 80°C and allowed to slowly cool to room temperature, before immobilization on gold surfaces. Such pre-heating and cooling is required to maintain the structural robustness of the aptamer for binding to the target molecules.[11]

2.2.3 Electrode/Substrate Preparation

The gold-coated slides (2.5 × 2.0 cm^2) were cleaned by dipping in a "piranha solution" (3:1 mixture of concentrated sulfuric acid and 30% hydrogen peroxide) for 5 min at about 90 °C. *[CAUTION: piranha reacts violently with organic solvents, and should be handled with extreme caution.]* They were rinsed thoroughly with deionized water and dried under N_2 afterwards.

Self-assembled monolayers (SAMs) of 11-mercaptoundecanoic acid on gold were prepared by immersing clean gold slides in a solution of 11-mercaptoundecanoic acid in 95% ethanol for 12 h. After adsorption, the gold slides were cleaned with ethanol and dried under N_2.[12]

Thiol-modified DNA strands were immobilized on clean gold substrates by spreading ~80 μL of 1 to 5 μM in immobilization buffer (**I-B**: 20 mM Tris-HCl / 0.1 M

NaCl/ 5 mM $MgCl_2$ at pH 7.5) for 12h. After modification, the sample was rinsed with 10 mM Tris-HCl buffer at pH 7.4 and immersed in 1.0 mM MCH solution for 30 min (for removing non-specifically adsorbed DNA strands on the gold surface), rinsed again with 10 mM Tris-HCl buffer (pH 7.4) and water, and dried under N_2 before characterization.

For the detection, 100 μL of lysozyme solution of varying concentration (in I-B buffer) was dropped onto the DNA-modified gold electrode. The sample was kept for an hour followed by incubation with wash buffer (**W-B**: 20 mM Tris-HCl/ 0.1 M NaCl / 5 mM $MgCl_2$ / 1.0% (v/v) Tween 20 at pH 7.5) for 20 min. The sample was finally rinsed with 10 mM Tris-HCl at pH 7.4 before characterization.

2.2.4 Electrochemical Measurements

Cyclic voltammetry was performed with a μAutolab II potentiostat / galvanostat (EcoChemie B.V., Utrecht, Netherlands). A single-compartment, three-electrode Teflon cell was used for the electrochemical measurements. DNA-modified gold slides were used as working electrodes and pressed against an O-ring seal at the cell bottom (with an exposed area of 0.66 cm^2). A Ag | AgCl | 3M NaCl electrode was used as reference electrode, and a Pt wire was used as the counter electrode.

Electrochemical measurements of DNA-modified electrodes were performed either in 5μM $[Ru(NH_3)_6]Cl_3$ in 10 mM Tris-HCl buffer at pH 7.4 or in 100 μM $K_3[Fe(CN)_6]$ in 10 mM Tris-HCl buffer / 0.1M NaCl / 5mM $MgCl_2$ at pH 7.4.

2.3 Results and Discussion

2.3.1 Electrochemical Response of Redox Ions on Bare and SAM-Modified Gold Electrodes

Alkanethiols mimic biomolecular self-assembly processes by spontaneously forming organized monolayer films on noble metal surfaces.[13,14] These organic films provide an effective method to control chemical and physical properties of electrode surfaces and have potential applications in biosensing, biomimetics, corrosion inhibition and wetting studies.

It has been shown experimentally that long-chain 11-mercaptoundecanoic acid molecules form a closely packed SAM on gold. The surface is uniformly covered with a layer of thiol molecules and the molecules on the surface are oriented with the –COOH groups projecting towards the electrolyte solution.[15,16] Monolayers of 11-mercaptoundecanoic acids on gold are model systems for DNA-modified surfaces, as they possess negative charges as well at the surface (as a result of the –COOH ionization).[15]

Figure 2.1 shows the representative cyclic voltammetric (CV) responses of 1.0 mM $[Fe(CN)_6]^{3-}$ in 0.1 M KCl at bare and SAM-modified gold electrodes. A well-defined reversible electrochemical response of $[Fe(CN)_6]^{3-}$, i.e. a pair of symmetric redox peaks corresponding to the reduction of $[Fe(CN)_6]^{3-}$ and re-oxidation of $[Fe(CN)_6]^{4-}$, has been observed at bare gold electrodes. A dramatic decrease of the peak currents has been observed after the electrode was modified with the SAMs. As indicated in Figure 2.1, the CV curve (dashed line) for a SAM-modified electrode shows only capacitive current. This is partly due to the decrease of the interfacial electron transfer rate when electrons are tunneling through densely-packed organic monolayers on the gold surface.[17] At

neutral pH, the carboxylic functional groups are negatively charged, due to ionization. The negatively charged surface repels the redox anions, $[Fe(CN)_6]^{3-}$, from the electrode, in addition to the blocking effect by the oriented alkyl chains. Therefore, the redox peaks of $[Fe(CN)_6]^{3-}$, which depend on the ion diffusion to and reduction at the gold electrodes, disappeared upon modification with the SAMs.

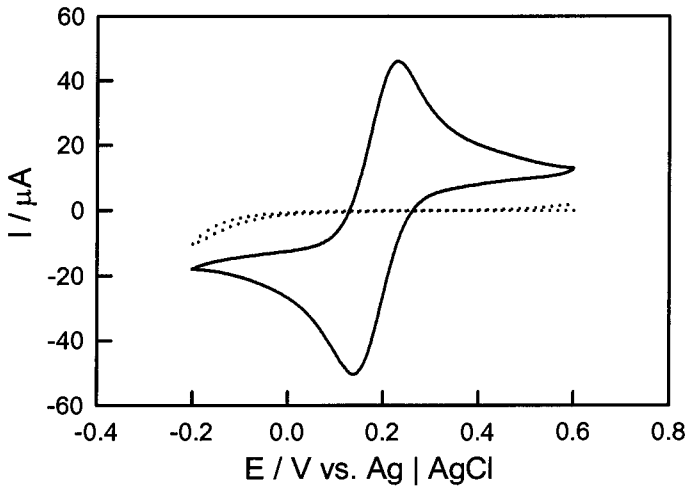

Figure 2-1 CVs of 1 mM $[Fe(CN)_6]^{3-}$ in 0.1 M KCl on bare (solid line) and SAM-modified (dashed line) gold electrodes, respectively. The scan rate was 100 mV/s.

We also tested the electrochemical behavior of a redox cation, $[Ru(NH_3)_6]^{3+}$, on these SAM-modified electrode surfaces. In contrast to the CVs of $[Fe(CN)_6]^{3-}$, the decrease of the redox peaks of $[Ru(NH_3)_6]^{3+}$ at SAM-modified electrodes is limited, but still evident as shown in Figure 2.2.

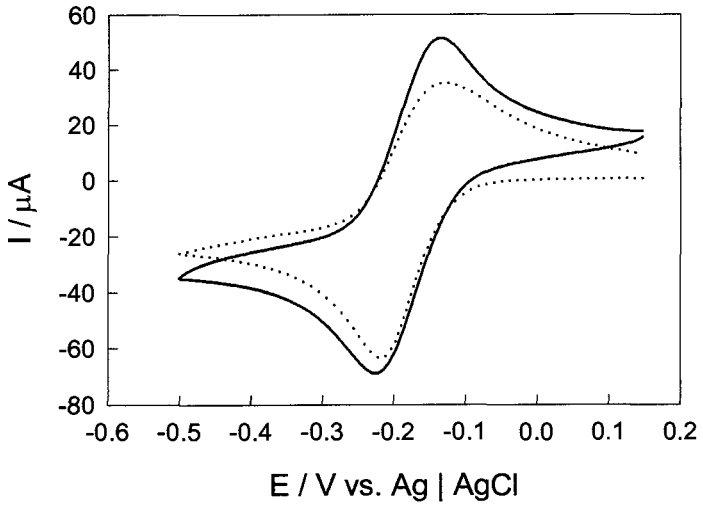

Figure 2-2 CVs of 1.0 mM $[Ru(NH_3)_6]^{3+}$ in 0.1 M KCl on bare (solid line) and SAM-modified (dotted line) gold electrodes, respectively. The scan rate was 100 mV/s.

As discussed above, 11-mercaptoundecanoic acids form highly ordered monolayers on gold surfaces, which in principle should also block the redox process of $[Ru(NH_3)_6]^{3+/2+}$. In contrast to the experiment with $[Fe(CN)_6]^{3-}$, there is an electrostatic attraction between these positively charged ions and the negatively charged functional groups on the surface. Such electrostatic interaction between the monolayer head group and the redox cation may dominate the electrode reaction.[18] The negatively charged surface hinders the reduction of negatively charged $[Fe(CN)_6]^{3-}$, but scarcely prevents the reduction of positively charged $[Ru(NH_3)_6]^{3+}$. Higher concentrations of cations accumulated at the monolayer surface may disturb the well-packed monolayer structure, particularly under potential scan. These factors may contribute to the fact that the redox response of $[Ru(NH_3)_6]^{3+}$ decreases only slightly at a SAM- modified electrode compared

with that at a bare-gold electrode. Nevertheless, this experiment should have been repeated for a more reliable explanation.

In summary, the redox behavior of $[Fe(CN)_6]^{3-}$ and $[Ru(NH_3)_6]^{3+}$ on bare and SAM-modified gold electrodes showed that electrostatic interactions between the redox anions / cations in solution and on electrode surfaces govern their electrochemical behavior. These electrochemical investigations of negatively charged SAM surfaces provide a valuable model system to study DNA-modified gold electrodes, which are similarly charged due to the anionic phosphate backbone.

2.3.2 Electrochemical Response of $[Fe(CN)_6]^{3-}$ on anti-Lysozyme Aptamer-Modified Gold Surfaces.

We expect that the redox behavior of $[Fe(CN)_6]^{3-}$ on DNA-modified gold electrodes would show some similarity to that of SAM-modified surfaces. Figure 2.3A shows the representative CVs of 0.1 mM $[Fe(CN)_6]^{3-}$ on the aptamer-modified gold electrodes before and after incubation in 20 μg/mL lysozyme solutions.

As shown in Figure 2.3B, the phosphate backbone of the DNA strands is negatively charged at neutral (physiological) pH; therefore, the modified electrode surface would repel the redox anions. However, unlike long-chain 11-mercaptoundecanoic acid, DNA molecules with the aptamer sequence may not form a densely packed monolayer on a gold surface. Therefore, the heterogeneous electron transfer between $[Fe(CN)_6]^{3-}$ in solution and the electrode cannot be completely blocked. The CV curves observed in this case (Figure 2.3A, dotted line) still show the redox peaks, although they are significantly smaller than those on bare gold electrodes. The

experiment should have been done with 1.0 mM $[Fe(CN)_6]^{3-}$ for a direct comparison with the CV responses on bare gold (Fig. 2.2, 2.3).

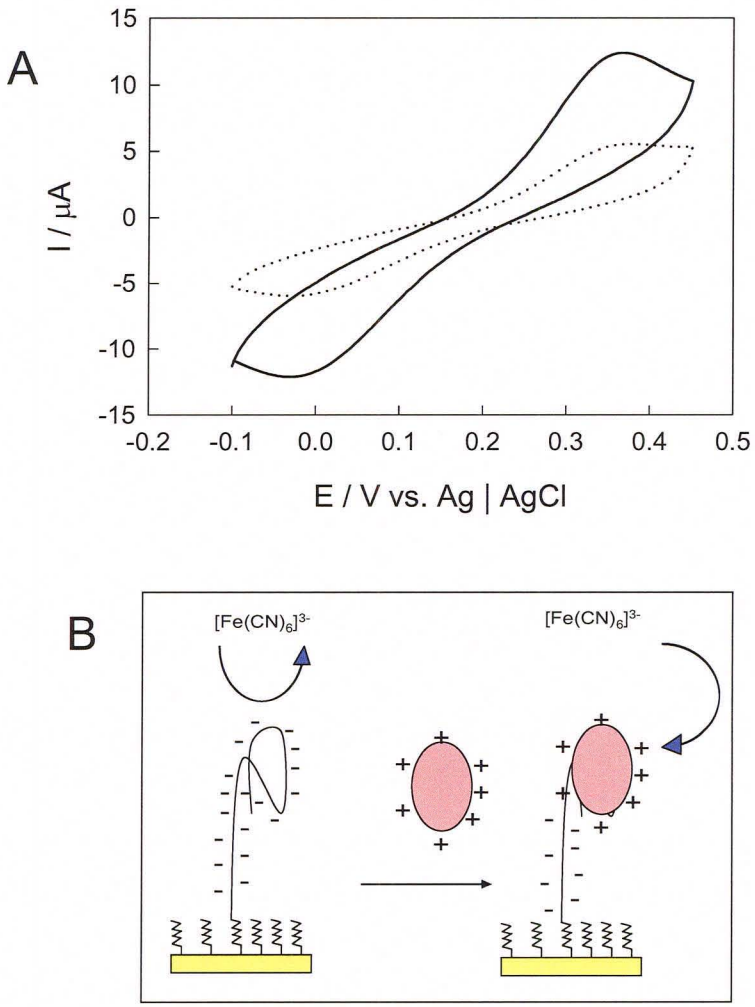

Figure 2-3 **(A) Cyclic voltammograms of 0.1 mM $[Fe(CN)_6]^{3-}$ on an aptamer-modified gold surface before (dotted line) and after (solid line) incubation with 20 µg/mL lysozyme. The scan rate was 100 mV/s. (B) Schematic representation of the anti-lysozyme aptamer-modified gold electrode before and after binding with lysozyme, in the presence of $[Fe(CN)_6]^{3-}$ in solution. After lysozyme binding, the surface charge is reduced, and hence, the repulsion between the surface and the $Fe(CN)_6]^{3-}$ in solution decreases.**

Lysozyme is a spherical protein with a diameter of 4 nm; at neutral pH the overall net charge of lysozyme is +7.[19] Binding of lysozyme to the aptamer-modified gold electrode should reduce the negative surface charge (contributed by the DNA backbone). We believe that a reversal of surface charge (i.e., from negative to positive) may not be possible due to the length of the oligonucleotide (42-mer) in comparison with the positive charge of each protein. This means that, upon binding of lysozyme to the aptamer-modified electrode, there is not enough positive charge from lysozyme, to create an excess positive charge on the surface. However, a decrease of the overall negative charge on the surface by lysozyme will promote the interfacial electron transfer reaction between the redox anions in solution and the electrode surface. This is reflected by the increase of the redox current in the CV as shown in Figure 2.3A (solid line). The CV responses obtained here are in agreement with the results described by Rodriguez et al.[11] Their impedance spectroscopic study showed that the electron transfer resistance decreased after binding of the protein to the aptamer-modified electrode.

We found that the reproducibility of this experiment is problematic, partially because we are looking at the effect of surface charge on the redox behavior of diffusing species in solution; therefore a quantitative detection of lysozyme is not practical based on votammetric studies of redox anions in solution.

2.3.3 Electrochemical Response of $[Ru(NH_3)_6]^{3+}$ on Aptamer-Modified Gold Electrodes

The drawback of the $[Fe(CN)_6]^{3-}$ method described above, directed us to use a different redox system to study the binding process of lysozyme to aptamer-modified gold electrodes. When the aptamer-modified surface is exposed to a solution containing

$[Ru(NH_3)_6]^{3+}$, the redox cations bind electrostatically (Figure 2.4A) to the negatively charged phosphate backbone by replacing the native charge compensation ions (Na^+), and reach an ion exchange equilibrium.

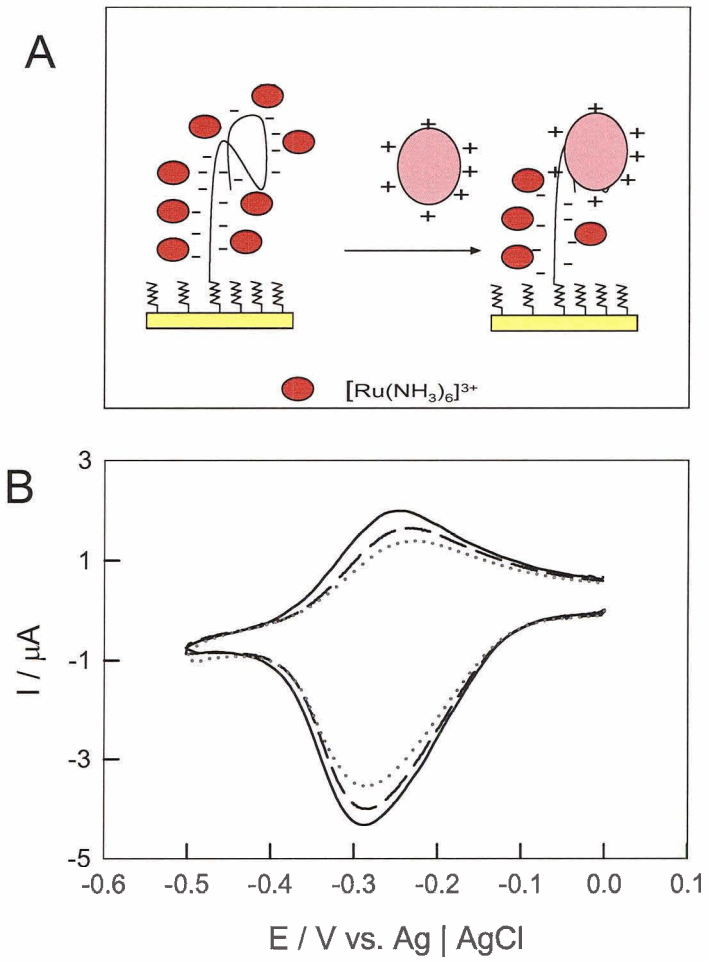

Figure 2-4 **(A) Schematic representation of the aptamer-modified gold electrode before and after binding with the lysozyme, in the presence of $[Ru(NH_3)_6]^{3+}$ in solution. (B) CVs of 5.0 µM $[Ru(NH_3)_6]^{3+}$ on an aptamer-modified gold surface before (solid line) and after incubation with 50 µg/mL (dashed line) and 100 µg/mL (dotted line) lysozyme . The scan rate was 100 mV/s.**

A well defined redox process of surface-bound $[Ru(NH_3)_6]^{3+}$ can be observed, as shown in Figure 2.4 B (solid line). The quantity of the surface-bound cations can be determined by integration of the redox peaks, and it can be used to determine the surface density of DNA strands.[6, 20]

As mentioned previously, upon binding of lysozyme (that is positively charged) to the aptamer-modified gold electrodes, the surface charge density would decrease, which should shift the equilibrium of the $[Ru(NH_3)_6]^{3+}$ ions bound to the surface and those in solution. This, indeed, is observed as a decrease of the redox peaks of $[Ru(NH_3)_6]^{3+}$ in the CV measurements (Figure 2.4B); upon adding lysozyme to the solution, the peak currents (and in turn the peak areas) significantly decrease (Table 2-1).

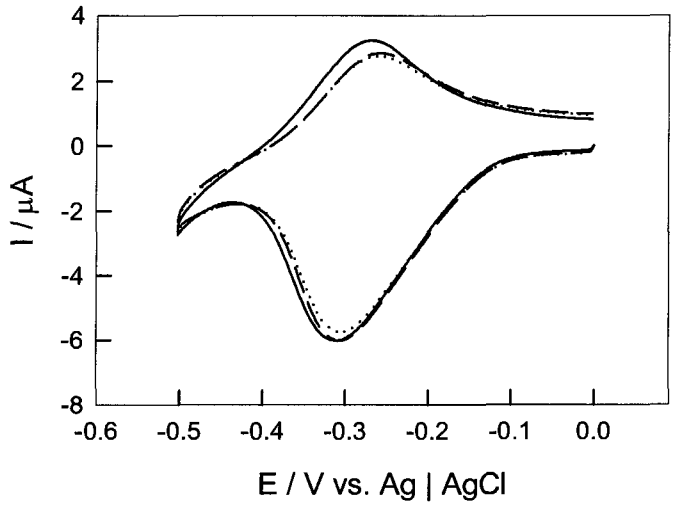

Figure 2-5 **Cyclic Voltammograms of 5.0 μM $[Ru(NH_3)_6]^{3+}$ on gold surface modified with anti-lysozyme aptamer before (solid line) and after incubation with 200 μg/mL (dashed line) and 600 μg/mL (dotted line) cytochrome c. The scan rate was 100 mV/s. No significant change in the integrated charge of the reduction peak was observed.**

It is important to investigate the specificity of aptamer-modfied gold electrodes for the detection of lysozyme. For this reason, another protein, cytochrome c, with similar isoelectric point (pI ~ 11) and size (12 kDa), was used as a control.[21] It was found that addition of cytochrome c to the solution produces no significant changes in CV response (up to 600 μg/mL) of aptamer-modified gold electrodes (Figure 2.5 and Table 2-2). These results indicate cytochrome c does not bind to the aptamer-modified gold electrodes in the aptamer-ligand interaction fashion.

It is more important to evaluate the detection limit and response range of these aptamer sensors towards lysozyme. We take the relative charge decrease as quantitation measure. Figure 2.6 shows the dependence of the CV response on the concentration of lysozyme, in which the ratio of $\frac{\Delta Q}{Q_i} = \frac{(Q_i - Q)}{Q_i}$ is a function of protein concentration, where Q_i and Q refer to the charges obtained by integration of the reduction peak of $[Ru(NH_3)_6]^{3+}$ in the CV before and after incubation with lysozyme, respectively. The data presented here (Table 2-1 and 2-2) are from three sets of experiments (i.e., with different electrodes) with a relative uncertainty for calculation of at least 10%. We found that with this method, lysozyme concentrations as low as 0.5 μg/mL may be detected, which is about ten times better than that reported by Rodriguez et al. using electrochemical impedance spectroscopy.[11]

Table 2-1 **Integrated charge of the reduction peak for $[Ru(NH_3)_6]^{3+}$ on aptamer-modified surfaces upon addition of lysozyme.**

	[Lysozyme] (μg/mL)	Q_i (C)	Q(C)
Electrode A	0	8.271×10^{-6}	
	0.5		7.998×10^{-6}
	5.5		7.611×10^{-6}
Electrode B	0	6.416×10^{-6}	
	20		5.252×10^{-6}
	120		5.002×10^{-6}
	320		4.294×10^{-6}
Electrode C	0	6.547×10^{-6}	
	10		5.890×10^{-6}
	60		4.789×10^{-6}

Table 2-2 **Integrated charge of the reduction peak for $[Ru(NH_3)_6]^{3+}$ on aptamer-modified surfaces upon addition of cytochrome c.**

	[Cytochrome C] (μg/mL)	Q_i (C)	Q (C)
Electrode D	0	7.395×10^{-6}	
	200		6.853×10^{-6}
	600		6.765×10^{-6}

In contrast to a regular sensor response, it has been observed that at higher protein concentrations, there is a steady increase in the signal. This could be explained as follows: the ratio of protein to aptamer on the surface is 1:1. At higher protein concentrations, the non-specific binding between the aptamer and protein due to electrostatic interaction may contribute to the decrease in the integrated charge of the reduction peak area, i.e., more $[Ru(NH_3)_6]^{3+}$ will be replaced.

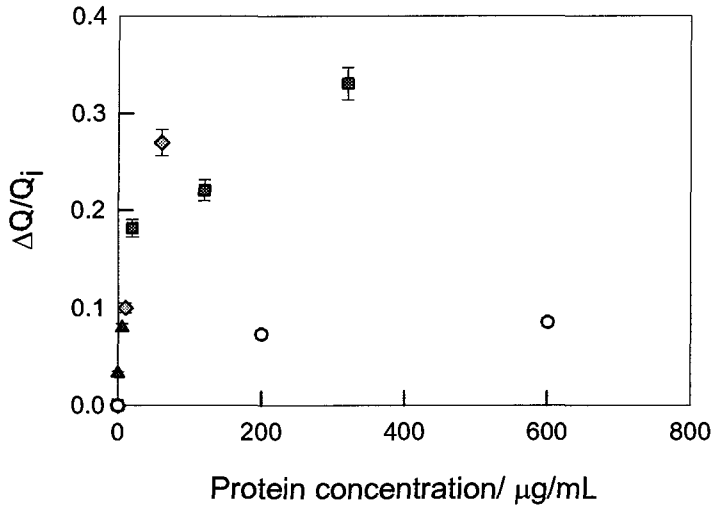

Figure 2-6 Decrease in the integrated charge (reduction peak) as a function of lysozyme concentration. Cytochrome c (open circles) was used as a control.

2.3.4 Correlation Between Sensor Sensitivity and Aptamer Surface Density

We have now confirmed that the voltammetric response of redox cations on aptamer-modified electrodes, before and after incubation with lysozyme, can be used as a quantitative measure for the detection of lysozyme. It is important to optimize the sensor performance, i.e., to improve the sensitivity and selectivity. One of many factors that could be influential is the density of aptamers on the electrode surface.

For this purpose, gold electrodes modified with different surface densities of aptamers were prepared (Table 2.3). This can be achieved by incubating at different DNA concentrations (0.1 – 10 μM) on the gold surfaces, by varying the immobilization time (10 s – 24 hrs) and by treating the surfaces with MCH at high concentration (1 mM). However, the uncertainty in the calculation of the integrated charge of redox cations as well as the surface density is relative high (> 15 %) and has not been reproduced.

Table 2-3 **Integrated charge of the reduction peak for $[Ru(NH_3)_6]^{3+}$ on aptamer-modified surfaces, the corresponding surface density of aptamer and the integrated charge after addition of 20 μg/mL of lysozyme**

Q_i (C)	$\Gamma_{aptamer}$ (molecules/cm^2)	Q (C)
1.159×10^{-6}	1.065×10^{12}	1.132×10^{-6}
3.154×10^{-6}	2.211×10^{12}	2.448×10^{-6}
6.416×10^{-6}	4.498×10^{12}	5.252×10^{-6}
1.182×10^{-6}	8.286×10^{12}	1.055×10^{-6}

Figure 2-7 shows a correlation between the sensor signal, $\frac{\Delta Q}{Q_i}$, and surface density of aptamers, Γ_{DNA}, on gold surfaces when the modified electrodes were incubated with the same concentration of lysozyme (20 μg/mL).

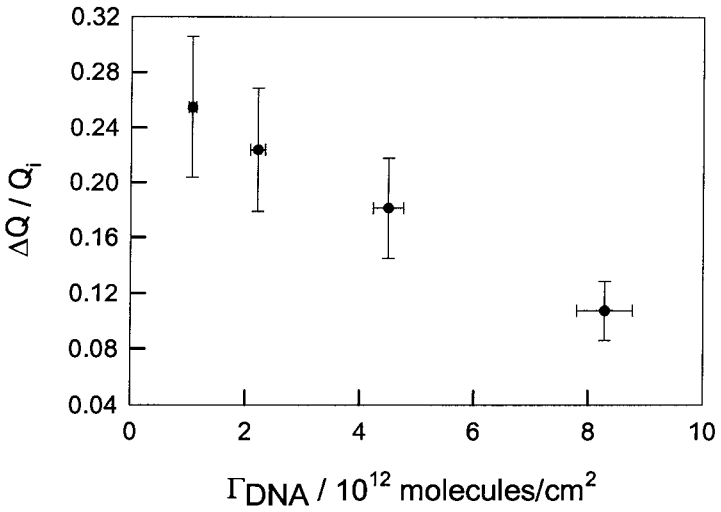

Figure 2-7 Sensor signal versus surface density of aptamers on gold electrode surface.

The result (Figure 2.7) shows that the sensor sensitivity is clearly dependent on the aptamer surface density. There is an apparent decrease in the sensor signal with the increase in the aptamer surface density. At higher surface density, we believe binding of lysozyme to the aptamer is hindered due to spatial restriction for the DNA strands to fold into the aptamer configuration for binding to the protein, which is fairly big (4 nm in diameter). For lower surface densities, this is no longer a concern. However, for lower surface densities, the electrochemical response of $[Ru(NH_3)_6]^{3+}$ bound to the aptamer backbone is weak, and hence the integrated charge of the reduction peak in the CV is difficult to quantify. Therefore, we believe that the ideal surface density for this aptamer sensor is around 4×10^{12} molecules / cm^2.

2.4 Conclusion

The present study demonstrates that simple electrochemical methods are capable of monitoring the binding of protein to an aptamer-modified surface. The binding event can be detected as a decrease in the integrated charge of the surface-bound $[Ru(NH_3)_6]^{3+}$ cations. The detection limit for lysozyme is as low as 0.5 μg/mL. However, the response at high concentrations is complex (involving non-specific, electrostatic interactions between the protein and the anionic DNA backbone). A correlation between the sensor sensitivity and the aptamer surface density has been observed.

2.5 References

1. For examples of DNA-modified surfaces, see: (a) Kelley, S. O.; Jackson, N. M.; Hill, M. G.; Barton, J. K. *Angew. Chem. Int. Ed.* **1999**, *38,* 941-943. (b) Kelley, S. O.; Barton, J. K.; Jackson, N. M.; Hill, M. G. *Bioconjugate Chem.* **1997,** *8,* 31-37. (c) Pang, D. W.; Abruña, H. D. *Anal. Chem.* **1998,** *70,* 3162-3169. (d) Herne, T. M.; Tarlov, M. J. *J. Am. Chem. Soc.* **1997,** *119,* 8916-8920.

2. For aptamer sensors, see (a) Nutiu, R.; Li, Y. *J. Am. Chem. Soc,* **2003,** *125,* 4771-4778. (b) Stojanovic, M. N; Kolpashchikov, D. M. *J. Am. Chem. Soc. 2004, 126,* 9266-9270. (c) Hoppe-Seyler, F.; Butz, K. *J. Mol. Med.* **2000,** *78,* 426-430. (d) Fahlman, R. P.; Sen, D. *J. Am. Chem. Soc.* **2002,** *124,* 4610-4616.

3. (a) Tuerk, G.; Gold, L.; *Science* **1990,** *249,* 505-510; (b) Ellington, A. D.; Szostak, J. W.; *Nature* **1990,** *346,* 818-822.

4. (a) Merino, E. J.; Weeks, K. M. *J. Am. Chem. Soc.* **2003,** *125,* 12370-12371; (b) McCauley, T. G.; Hamaguchi, N.; Stanton, M. *Anal. Biochem.* **2003,** *319,* 244-250.

5. (a) Liu, J; Lu, Y. *Anal. Chem.* **2004,** *76,* 1627-1632; (b) Pavlov, V.; Xiao, Y.; Shylabovsky, B.; Willner, J. *J. Am. Chem. Soc.* **2004,** *126,* 11768-11769.

6. (a) Yu, H.-Z.; Luo, C-Y; Sankar, C. G.; Sen, D. *Anal. Chem.* **2003,** *75,* 3902-3907: (b) Su, L.; Sankar, C. G.; Sen, D.; Yu, H.-Z. *Anal. Chem.* **2004**, *76*, 5953-5959. (c) Su, L.; Sen, D.; Yu, H.-Z. *Analyst* **2006**, *131*, 317-322:

7. Stryer, L. *Biochemistry* 3rd Edition, W. H. Freeman and Company, New York, **1998,** pp 201-203.

8. Cox, J. C.; Ellington, A.D. *Bioorg. Med. Chem.* **2001**, *9*, 2525-2531.

9. Cox, J. C.; Hayhurst, A.; Hesselberth, J.; Bayer, T. S.; Georgiou, G.; Ellington, A. D. *Nucleic Acids Res.* **2002,** *30,* e108.

10. Kirby, R.; Cho, E. J.; Gehrke, B.; Bayer, T.; Park, Y. S.; Neikirk, D. P.; McDevitt, J. T.; Ellington, A. D.; *Anal. Chem.* **2004,** *76,* 4066-4075

11. Rodriguez, M; Kawde, A-N; Wang, J. *Chem. Comm.* **2005,** 4267-4269.

12. Aqua, T.; Naaman, R.; Daube, S. S. *Langmuir* **2003**, *19*, 10573-10580.

13. Schreiber, F.; Eberhardt, A.; Leung, T. Y. B.; Schwartz, P.; Wetterer, S. M.; Lavirich, D. J. ; Berman, L.; Fenter, P.; Eisenberger, P. ; Scoles, G. *Phys. Rev. B.* **1998,** *57,* 12476-12481.

14. Poirier, G.E. *Langmuir* **1999,** *15,* 1167-1175.

15. Godin, M.; Williams, P.J.; Tabard-Cossa, V.; Laroche, O.; Beaulieu, L.Y.; Lennox, R.B.; Grutter, P. *Langmuir* **2004,** *20,* 7090-7096.

16. Schwartz, D.K. *Annu. Rev. Phys. Chem.* **2001,** *52,* 107-137.

17. Yu, H. Z. *Anal. Chem.* **2001**, *73*, 4743-4747.

18. Takehara, K.; Takemura, H.; Ide, Y. *Electrochimi. Acta,* **1994,** *39,* 817-822.

19. RCBS, Protein Data Bank, http://www.rcsb.org/pdb/static.do?p=Viewers/QuickPDB/quickPDBApplet.jsp

20. Steel, A. B.; Herne, T. M.; Tarlov, M., J.; *Anal. Chem.* **1998**, *70*, 4670-4677

21. (a) http://en.wikipedia.org/wiki/Cytochrome_c; (b) Voet, D. and Voet, J.; *Biochemistry* 3rd Edition, John Wiley and Sons, **2004**.

CHAPTER 3
PRELIMINARY ELECTROCHEMICAL STUDIES OF DNA-MODIFIED SURFACES WITH ORGANIC INTERCALATORS

In Chapter 2, we have demonstrated a simple electrochemical protocol to monitor and quantify the protein-aptamer interactions on surfaces using electrostatic binding of $[Ru(NH_3)_6]^{3+}$ redox markers. This chapter describes our attempt to use DNA intercalators as redox markers for electrochemical detection of analytes.

3.1 Introduction

Intercalators are molecules that intercalate into the space between two adjacent base pairs of DNA double helices. These molecules are mostly polycyclic, aromatic and planar. The most intensively studied DNA intercalators include ethidium bromide, daunomycin and methylene blue, which have been used by Barton and coworkers to study long distance electron transfer through DNA.[1-5] The intercalator was not used in the assay to report the amount of DNA or whether it is double-stranded versus single-stranded. Instead, it was used to examine whether DNA base pair stacking acts as a mediator for charge transport to the intercalator bound to the top of the film from the electrode surface.

Gooding and co-workers have used intercalators to detect target strands.[6-8] A mixed SAM of single-stranded DNA (ssDNA), thiolated at the 3'-end with MCH, was

formed on a gold surface. The ssDNA-modified surface was exposed to a solution containing 9,10-anthraquinone-2,6-disulfonic acid (AQDS). No voltammetric responses corresponding to the surface-bound intercalators were obtained for the ssDNA-modified surface. Upon hybridization with the complementary strands and upon incubation in AQDS solution, clear redox peaks were obtained, consistent with the oxidation and reduction of AQDS.[6] The absence of AQDS response for ssDNA-modified surfaces is due to the fact that AQDS does bind specifically to the single-stranded DNA.[7] No electrochemical behavior was observed when the ssDNA-modified electrode was exposed to a non-complementary sequence. Inspired by the ideal electrochemistry of AQDS, ease of operation (as no synthesis is required), and negligible non-specific binding, we decided to explore the use of AQDS as a redox probe to study aptamer-analyte binding. A representative of this idea is shown in Figure 3.1. This is also complementary with the biochemical experiments carried out in Dr. Sen's lab for testing these deoxyribosensors, in which a covalently attached AQ group was used as the photoinitiator.[9]

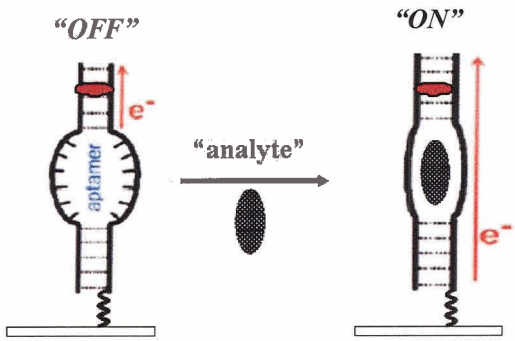

Figure 3-1 **Schematic representation of AQDS-intercalated deoxyribosensors. The charge transfer between AQDS and the electrode is "cut-off" in the absence of the analyte ('OFF' state) and "resumed" in the presence of the analyte ('ON' state).**

3.2 Experimental Section

3.2.1 Materials

The synthetic oligonucleotides, HO-$(CH_2)_6$-S-S-$(CH_2)_6$-O-5'-TCG ATC TGA CGT CAG CTA AA-3' and 5'-TTT AGC TGA CGT CAG ATC GA-3' were purchased from Core DNA Services Inc. (Calgary, AB). The 5'-thiol modifier was obtained from Glen Research (Sterling, VA).

Glass slides coated with 5 nm chromium and 100 nm gold were obtained from Evaporated Metal Film (EMF) Inc. (Ithaca, NY). 9,10- Anthraquinone-2,6-disulfonic acid (AQDS), 6-Mercapto-1-hexanol (MCH), hexaammine ruthenium (III) chloride (98%), and 11-mercaptoundecanol were from Sigma and used as received. Deionized water (>18.3 MΩ.cm) was from a Barnstead Easy Pure UV/UF compact water system (Dubuque, IA).

3.2.2 DNA Purification

The disulfide-modified oligonucleotide was purified by reverse-phase HPLC on a Gemini 5-μm C18/110 Å column (Phenomenex, Torrance, CA), eluting with a gradient of 0.1 M triethylammonium acetate (TEAA) / CH_3CN (20:1) and CH_3CN at 1.0 mL/min. The sample was then treated with 10 mM tris(carboxyethyl)phosphine (TCEP) in 100 mM Tris buffer at pH 7.5 for 4 hours and desalted through a MicroSpin G-50 columns (G-50 Sephadex) to yield thiol-modified single-stranded DNA (HS-DNA), HS-$(CH_2)_6$-O-5'- TCG ATC TGA CGT CAG CTA AA-3'.

3.2.3 Electrode Preparation

The gold-coated slides (2.5 × 2.0 cm^2) were cleaned by dipping in a "piranha solution" (3:1 mixture of concentrated sulfuric acid and 30% hydrogen peroxide) for 5 min at about 90°C, as mentioned previously. They were rinsed thoroughly with deionized water and dried under N_2 afterwards.

Oligonucleotide was immobilized on clean gold substrates by spreading ~80 μL of 10 μM HS-DNA in immobilization buffer (1 M KH_2PO_4 at pH 4.5) for 2-3 hours. After modification, the sample was rinsed with 10 mM Tris-HCl buffer at pH 7.4 and immersed in 1 mM MCH solution for 30 min (for removing non-specifically adsorbed DNA strands), rinsed again with 10 mM Tris-HCl buffer at pH 7.4 and water and incubated in 1mM AQDS solution containing 0.2 M KCl / 50 mM KH_2PO_4 at pH 7.0 for 3 hours. Hybridization was performed by incubating the ssDNA-modified electrode with 15 μM complementary sequence in 1 M NaCl / 10 mM Tris-HCl at pH 7.0 for 6 hours followed by rinsing with 10 mM Tris buffer at pH 7.0. The dsDNA-modified electrode was incubated with AQDS solution overnight at room temperature. The electrode was rinsed with 10 mM Tris-HCl at pH 7.0 and water, followed by drying under N_2 before characterization.

3.2.4 Electrochemical Measurements

Cyclic voltammetry was performed with a μAutolab II potentiostat / galvanostat (EcoChemie B.V., Utrecht, Netherlands). A single-compartment, three-electrode Teflon cell was used for the electrochemical measurements. DNA-modified gold slides were used as working electrodes and pressed against an O-ring seal at the cell bottom (with an exposed area of 0.66 cm^2). An Ag | AgCl | 3 M NaCl electrode was used as reference

electrode, and a Pt wire was used as the counter electrode. Electrochemical measurements were carried out in 0.3 M KCl / 50 mM KH_2PO_4 / K_2HPO_4 at pH 7.0.

3.3 Results and Discussion

3.3.1 Electrochemistry of AQDS on Bare Gold Electrodes

Prior to investigating the redox behavior of AQDS on DNA-modified electrode surface, the electrochemistry of AQDS at bare gold, at a short-chain thiol (MCH) and at a long-chain thiol (1-mercapto-undecanol) modified electrode were investigated, respectively. Cyclic voltammograms of 1 mM AQDS solution in 50 mM phosphate buffer / 0.3 M NaCl at pH 7.0 at bare and modified electrodes are shown in Figure 4.2. At the bare gold electrode (solid line), AQDS showed reversible redox peaks with the formal potential ($E^{o'}$) of -411 mV (vs. Ag | AgCl) and a peak separation (ΔEp) of 86 mV, which is in agreement with literature.[10] At the MCH-modified gold electrode (dashed line), the redox peak currents remain only 1/3 of those at bare gold although $E^{o'}$ and ΔEp remain the same, indicating a partial suppression of the AQDS electrochemistry. A large amount of AQDS has been prevented from penetrating through the SAM towards the gold surface. Furthermore, when 11-mercaptoundecanol was used to modify the gold surface (dotted line), no redox peaks have been observed, indicating a complete suppression of the AQDS redox reaction. The repulsion of AQDS from the gold surface by the SAM is believed to be due to electrostatic repulsion between the negatively charged redox molecule and the negative dipole of the hydroxyl groups.[11]Long-chain thiols can form more densely packed monolayers on the gold surface than short-chain thiols. Therefore,

long-chain thiols are more effective in preventing the redox molecules from undergoing direct electrochemical reactions.

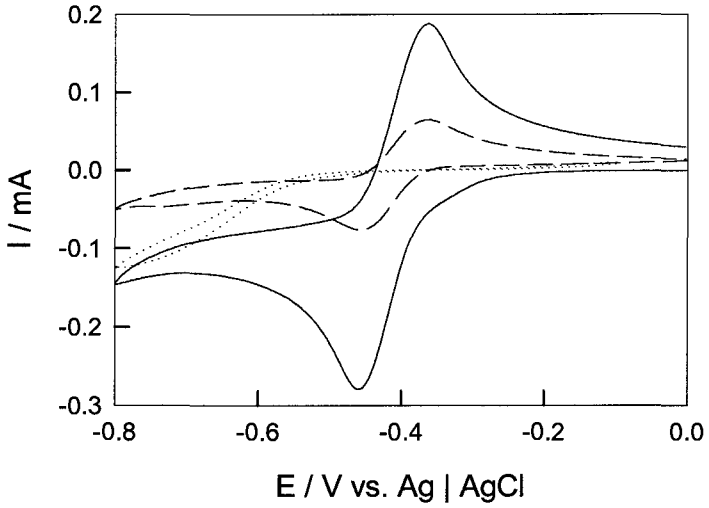

Figure 3-2 CVs of bare (solid line), MCH-modified (dashed line) and 1-mercaptoundecanol-modified (dotted line) gold electrode in 1mM AQDS in 0.2 M KCl and 50 mM phosphate buffer at pH 7.0. The scan rate was 100 mV/s.

3.3.2 Electrochemistry of AQDS on DNA-Modified Gold Electrodes

After the ssDNA-modified electrode was prepared, it is generally treated with 1 mM mercaptohexanol (MCH) solution. The purpose of the MCH is two-fold: first, to increase hybridization efficiency by preventing the DNA bases from nonspecifically associating with the gold electrode; and second, to restrict direct access of the AQDS to the electrode surface. Exposure of the ssDNA-modified electrode to the complementary target DNA will form the dsDNA-modified electrode.

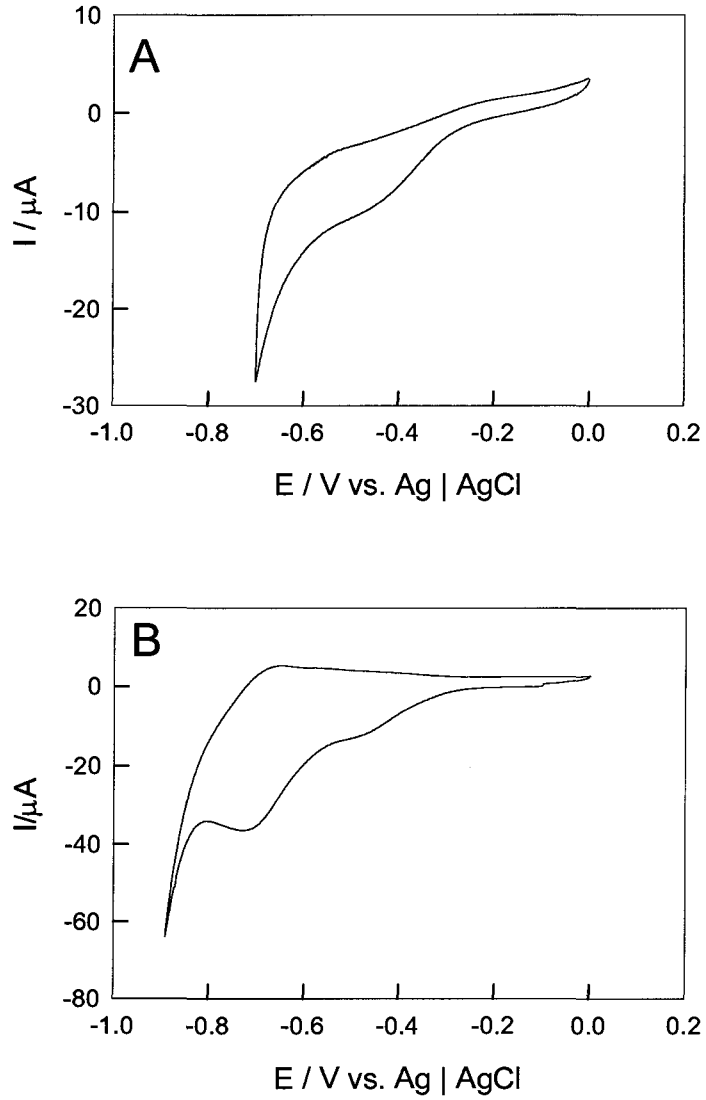

Figure 3-3 CVs for ssDNA-modified (A) and dsDNA-modified (B) gold electrode in 1mM AQDS in 0.3 M NaCl, 50 mM phosphate buffer at pH 7.0. The scan rate for both was 100 mV/s.

The electrochemical behavior of AQDS was investigated at both ssDNA- and dsDNA-modified electrodes in phosphate buffer after incubating the electrodes in 1 mM AQDS solution overnight (Figure 3.3). These CVs are more complex in comparison with

the solution experiments, as multiple peaks were observed and their assignments were challenging.

The first peak was observed at E°' of -411 mV in both cases, which is much smaller than the peak of AQDS at a MCH-modified electrode (Figure 3.2). The appearance of the second peak at -687 mV was only observed at the dsDNA-modified electrode. We believe this may be corresponding to the AQDS molecules that are intercalated to the dsDNA monaolayers; however, the peak was weak and is not always reproducible. In comparison, Gooding et al. reported more pronounced redox response with AQDS as intercalative redox labels, although the DNA sequence and experimental conditions were different from ours.[6-8]

They also proposed that the AQDS molecule penetrates only the very top of the DNA because of charge repulsion.[2-4] When hybridized, the DNA duplexes are rigid negatively charged rods projecting from the interface. For the molecule to intercalate onto the base closer to the electrode would require the negatively charged AQDS molecules to penetrate through a negative charged environment. Furthermore, the repulsive barrier of the interface for the second AQDS to intercalate become more extreme when a negatively charged AQDS molecule has already intercalated into the top of the DNA duplexes.

3.4 Conclusion

From the CV measurements, we did not observe significant differences between single-stranded and double-stranded DNA when AQDS molecules were used as intercalative redox labels. Further experiments including the change of the sequence and

experimental conditions are required to further illustrate the feasibility of this seemingly simple experimental approach.

3.5 References

1. Boon, E. M.; Barton, J. K. *Curr. Opin. Strucl. Biol.* **2002**, *12*, 320-329.
2. Kelley, S. O.; Barton, J. K.; Jackson, N. M.; Hill, M. J. *Bioconj. Chem.*, **1997,** *8*, 31-37.
3. Boon, E. M.; Salas, J. E.; Barton, J, K. *Nat Biotechnol* **2000**, *18*, 1096-1100.
4. Kelley, S. O.; Boon, E. M.; Barton, J. K.; Jackson, N. M.; Hill, M. G. *Nucleic Acids Res.* **1999**, *27*, 4830-4837.
5. Drummond, T. G.; Hill, M. G.; Barton, J. K. *Nature Biotech.* **2003,** *21,* 1192-1199.
6. Wong, E. L. S; Gooding, J. J; *Anal Chem.* 2003, **75**, 3845-52.
7. Wong, E. L. S.; Erohkin, P; and Gooding, J. J; *Electrochem. Commun.* **2004**, 6, 648-654.
8. Wong, E. L. S.; Gooding, J. J. *Anal Chem.* **2006,** *78,* 2138-2144.
9. Fahlman, R. P; Sen, D. *J. Am. Chem. Soc.* **2002,** *124,* 4610-4616.
10. Revenga, J.; Rodriguez, F.; Tijero, J. *J. Electrochem. Soc.* **1994**, *141*, 330-333.
11. Dai, Z.; Ju, H. *Phys. Chem. Chem. Phys.* **2001**, *3*, 3769-3773.

CHAPTER 4
SYNTHESIS OF FERROCENE-TERMINATED OLIGONUCLETIDES AND THEIR ELECTROCHEMICAL CHARACTERIZATION

This chapter describes the synthesis of an oligonucleotide covalently tethered to a ferrocene moiety, as a redox-active marker (Fc-DNA), and the electrochemical behavior of a Fc-DNA-modified gold electrode. This study is of practical importance for further development of DNA-based biosensors, because covalent bonding provides a more robust and simpler electrochemical redox labeling protocol.

4.1 Introduction

In the second chapter, a simple label-free voltammetric method for the detection of lysozyme by anti-lysozyme aptamer immobilized on gold surfaces has been reported. The method was based on the protocol developed in our laboratory.[1] Upon incubation with a solution containing a redox-active transition metal cation, like $[Ru(NH_3)_6]^{3+}$, an ion exchange equilibrium is established between cations present in solution and the native-charge compensation ions, mainly Na^+ and $Tris^+$, electrostatically associated with the negative DNA backbone.[1] In order to expand the electrochemical method to a wide range of application, covalently attaching a redox-active marker to oligonucleotide is essential.

DNA is electrochemically inert under moderate electrode potentials.[2] Armistead and Thorp have electro-catalytically oxidized guanine using inorganic metal complexes, and reported that electrochemical detection of target requires the use of exogenous reporter groups.[3] Nucleic acid probes tethered at one end to a solid surface are to date more than just tools for detecting targets in solution. They are also emerging as critical model systems for directly assessing the basic physical properties of DNA polymer chains as well as their specific interactions with other molecules. Particularly relevant examples for these studies are those single-stranded (ssDNA) or double-stranded (dsDNA) systems that attach a reporter molecule at the free end or at a precise location along its length. For instance, short dsDNA-modified electrodes containing guanine residues labeled with a redox intercalator act as an electron acceptor (e.g., anthracycline). This has proven to be a useful system for exploring on the nanometer-length scale, long-range electron transport through densely-packed duplex DNA monolayer films. Barton and coworkers have approached this technique by employing exogenous electro-catalytic species for amplification.[4] They also reported that the current flow through the double-helix is sensitive even to single base mismatches, paving the way for the direct electrochemical detection of point mutations.[5]

Long et al. have used covalently attached ferrocenyl labels to compare electron transfer rates through two DNA constructs with ferrocene units bound at two different positions.[6] Anne and coworkers have investigated the redox behavior of the ferrocene moiety attached to a ssDNA probe before and after hybridization with the complementary strand.[7]

Along the same line of exploration, the present work stems from our continued efforts to develop versatile electrochemical biosensors for molecular analytes by constructing conformational DNA-switches.[8] In this chapter, the synthetic procedures to covalently modify the oligonucleotide with a redox-active species, ferrocene will be described. The synthesized Fc-DNA was immobilized on a gold electrode surface for further electrochemical investigation. The Fc-DNA-modified electrode is of interest as it can be used for the electrochemical investigation of long-range charge transfer via DNA base pair or for the quantitative analysis of other molecules which may specifically bind to DNA, inducing a conformation change and therefore a variation of charge transfer rates/pathways.[8] This work represents a critical step in exploring electrochemical DNA/aptamer-binding assays for more specific biomedical analytes.

4.2 Experimental Section

4.2.1 Materials

The following synthetic oligonucleotides (a and b) were obtained from Core DNA Services, Inc. (Calgary, AB) without post-synthesis purification. The 5'-thiol modifier was obtained from Glen Research (Sterling, VA). Amino-terminated oligonucleotide [NH_2-DNA (a)] was used for the synthesis of ferrocene-terminated oligonucleotide [Fc-DNA]. SS-DNA (b) was used to generate thiolated DNA [HS-DNA] after the cleavage of the disulfide bond.

(a) NH_2-DNA: NH_2-$(CH_2)_6$-O-5'-TTT AGC TGA CGT CAG ATC GA-3'

(b) SS-DNA: HO-$(CH_2)_6$-S-S-$(CH_2)_6$-O-5'-TCG ATC TGA CGT CAG CTA AA-3'

Glass slides coated with 5 nm chromium and 100 nm gold were obtained from Evaporated Metal Film (EMF) Inc. (Ithaca, NY). Ferrocenecarboxylic acid (FcA), N-

hydroxysuccinimide (NHS), and dicyclohexanecarbodiimide (DCC) were bought from Sigma-Aldrich (Milwaukee, WI) and used as received. Deionized water (>18.3 MΩ.cm) was from a Barnstead Easy Pure UV/UF compact water system (Dubuque, IA).

4.2.2 Synthesis, Purification and Characterization of Ferrocene-Terminated DNA

Synthesis and purification of NHS ester of ferrocenecarboxylic acid (Fc-NHS-ester). The following synthesis procedure was adopted from the literature with slight modifcaitons.[9] (2.2 mmol, 0.5 g) of ferrocene carboxylic acid and (2.5 mmol, 0.29 g) of N-hydroxysuccinimide were dissolved in 20 ml of dioxane and stirred at room temperature; (2.5 mmol, 0.5g) of dicyclohexylcarbodiimide dissolved in 5 mL of dioxane was added drop by drop. The mixture was stirred in the dark at room temperature overnight. The solution was filtered twice to remove dicyclohexylurea, formed as a side product during the reaction. The filtrate was concentrated (using rot. evap.) to dryness, and the yellow solid obtained was dissolved in chloroform and purified by chromatography on a column with silica gel 60 (EMD). The product was eluted with chloroform and concentrated to dryness. During the entire process, the reaction vessel was covered with aluminum foil to protect it from light. The Fc-NHS ester product obtained was characterized by ^{1}H NMR ($CDCl_3$) and mass spectrometry and stored in the dark at 4°C until use.

Synthesis and purification of Fc-DNA. Oligonucleotide concentrations were determined by measuring the absorbance at 260 nm with a UV-visible spectrophotometer. NH_2-DNA (a) was purified by polyacrylamide gel electrophoresis (PAGE) and used for the coupling reaction adjusted from the literature.[9] NH_2-DNA (26 nmol) was dissolved in 20 μL of 0.5 M $NaHCO_3/Na_2CO_3$ buffer at pH 9.0. To this was added 6 μL of Fc-NHS-

ester (1.3 μmol) dissolved in dimethylsulfoxide (DMSO). The mixture was sonicated for 10 min and stirred in the dark at room temperature overnight. The coupling mixture was then diluted to 100 μL with 50 mM triethylammonium acetate (TEAA) buffer at pH 7.0 and desalted on a NAP-5 column (Pharmacia Sephadex G-25). The product was then purified by reverse-phase HPLC on a Gemini 5-μm C18/110Å column (Phenomenex, Torrance, CA).

Matrix-Assisted Laser Desorption Ionization Time-of-flight (MALDI-TOF) mass spectrometry. The MALDI-TOF mass spectrometry of self-synthesized Fc-DNA was performed in the Voyager DE Biospectrometry workstation. Samples were prepared as follows: to 2 μL Fc-DNA (>10 μM) in water, 2 μL 0.1 M diammonium hydrogen citrate (additive) in water and 4 μL of 6-aza-2-thiothymine (ATT, Matrix, Fluka) saturated in CH_3CN were added. Eight spots, each with 1 μL of Fc-DNA mixture were dried for the measurements.

4.2.3 Purification of SS-DNA and Cleavage of the Disulfide Bond to Generate HS-DNA

The sequence SS-DNA (b) was purified by reverse-phase HPLC on a Gemini 5-μm C18/110 Å column (Phenomenex, Torrance, CA), eluting with a gradient of 0.1 M triethylammonium acetate (TEAA) / CH_3CN (20:1) and CH_3CN at 1.0 mL/min. The sample was then treated with 100 mM DTT (dithiothreitol) in 10 mM Tris at pH 8.5 for 30 minutes and desalted through a MicroSpin G-50 column (G-50 Sephadex, Amersham) to yield HS-DNA, HS-$(CH_2)_6$-O-5'-TCG ATC TGA CGT CAG CTA AA -3'.

4.2.4 DNA Hybridization

DNA hybridization was done in solution. 10 μM HS-DNA was mixed with 15 μM Fc-DNA, in 10 mM Tris HCl / 0.1 M NaCl / 0.1 M $MgCl_2$ at pH 7.4. The mixture was heated to 90°C and then allowed to cool slowly to room temperature for 1 hr to form Fc-dsDNA.

4.2.5 Modification of Gold Electrode with HS-DNA-Fc

The gold-coated slides (2.5 × 2.0 cm^2) were cleaned by dipping in a 3:1 mixture of concentrated sulfuric acid and 30% hydrogen peroxide) for 5 min at about 90°C. They were rinsed thoroughly with deionized water and dried under N_2.

DNA-modified electrodes were prepared by dropping ~80 μL of the HS-dsDNA-Fc on each gold-coated slide and incubating at room temperature overnight. The electrodes were then rinsed with 10 mM Tris-HCl / 50 mM NaCl at pH 7.4 and dried under N_2.

4.2.6 Electrochemical Measurements

Cyclic voltammetry was performed with a μAutolab II potentiostat / galvanostat (EcoChemie B.V., Utrecht, Netherlands). A single-compartment, three-electrode Teflon cell was used for the electrochemical measurements. DNA-modified gold slides were used as working electrodes and pressed against an O-ring seal at the cell bottom (with an exposed area of 0.66 cm^2). A Ag | AgCl | 3M NaCl electrode was used as reference electrode, and a Pt wire was used as the counter electrode. The electrochemical measurements were done in 10 mM Tris-HCl/ 50 mM NaCl at pH 7.4.

4.3 Results and Discussion

4.3.1 Synthesis, Purification and Characterization of Fc-DNA

Before synthesis of Fc-DNA, ferrocenecarboxylic acid was activated by N-hydroxysuccinimide as described in the experimental section. Figure 4.1 shows the equation for the reaction.

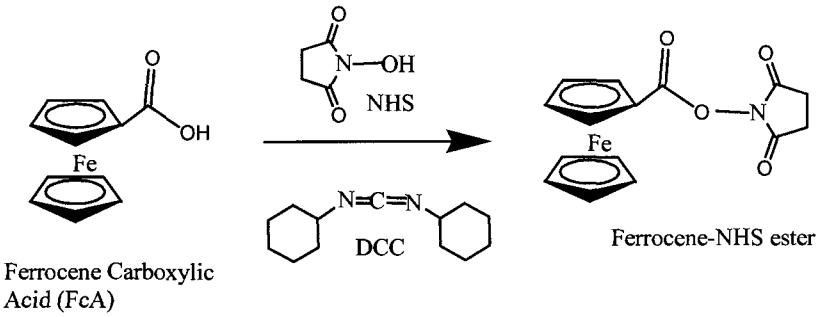

Figure 4-1 Reaction of ferrocenecarboxylic acid (FcA) with N-hydroxysuccinimide (NHS) in the presence of dicyclohexylcarbodiimide (DCC) to form the Fc-NHS-ester.

The obtained product was analyzed by mass spectrometry (Figure 4.2A). The measured mass of 327.0 is the same as the calculated mass of 327.02. Further analysis of the product by ^{1}H NMR ($CDCl_3$) (Figure 4.2B) shows peaks at δ = 2.9 (4H, s), 4.44 (5H, s), 4.6 (2H, m), 4.99 (2H, m), which confirm that the obtained product is Fc-NHS-ester. The yield of the product was calculated to be about 95%.

The purified Fc-NHS-ester was then used to link the ferrocene with oligonucleotides to form Fc-DNA in an aqueous solution containing 23% DMSO as described in the experimental part and in Figure 4.3. The solvent component was optimized according to the solubility of both NH_2-DNA and Fc-NHS-ester. The final product was purified first by a Nap-5 column to separate oligonucleotides from small

molecules (non- reacted Fc-NHS-ester etc.) and then by HPLC to separate Fc-DNA from unreacted NH_2-DNA. Figure 4.4 shows the HPLC chromatograph of NH_2-DNA before and after coupling with Fc-NHS-ester.

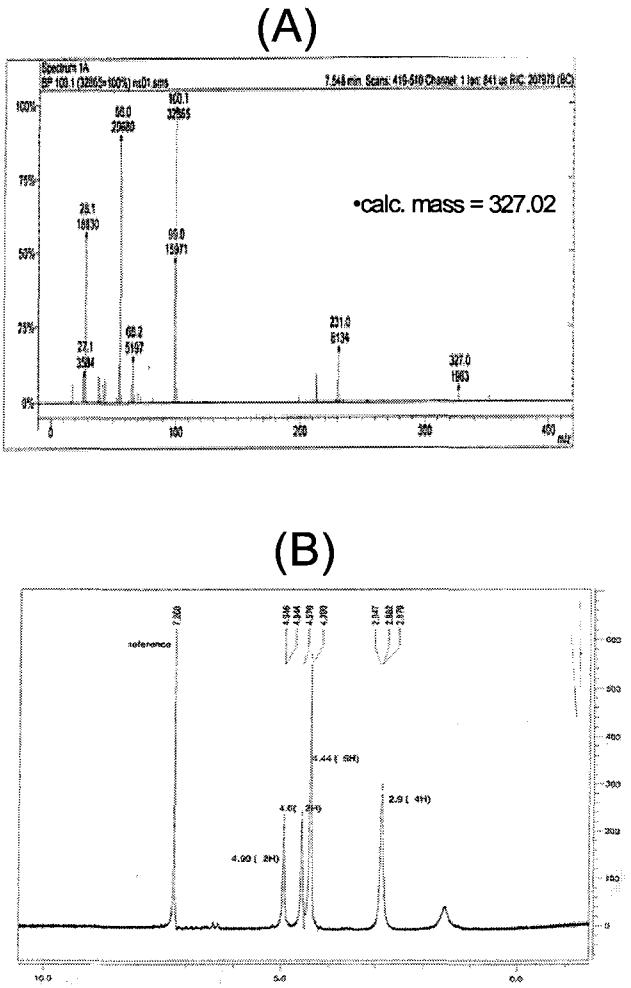

Figure 4-2 Mass spectrometry (A) and ^1H NMR ($CDCl_3$) (B) of the reaction product, Fc-NHS-ester, after the activation of ferrocenecarboxylic acid with N-hydroxysuccinimide.

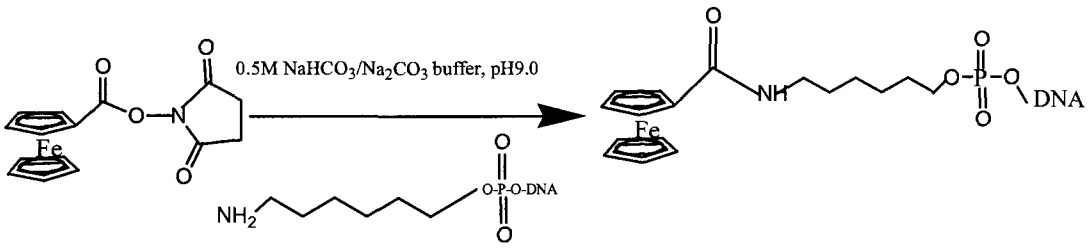

Figure 4-3 Coupling reaction of Fc-NHS-ester with NH_2-DNA to form Fc-DNA.

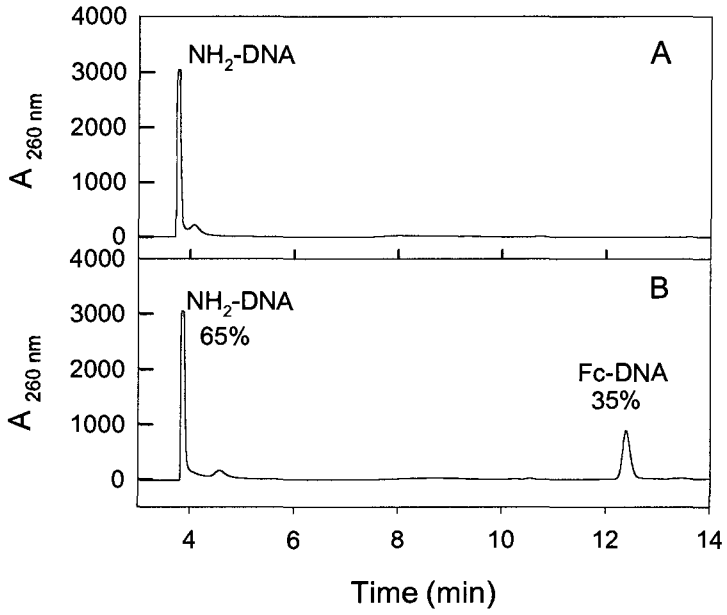

Figure 4-4 HPLC of NH_2-DNA before (A) and after (B) coupling with Fc-NHS-ester. The second peak at 12.4 min in (B) indicates the formation of Fc-DNA.

Before the coupling reaction, a sharp peak for NH_2-DNA at 3.7 min was observed. After the reaction, a second peak appeared at 12.4 min, which was supposed to be Fc-DNA. This peak was collected, subjected to speed vacuum to dryness and characterized with MALDI-TOF mass spectrometry as shown in Figure 4.5. The

measured mass of 6527.4 is close to the calculated mass of 6522.7, indicating the final product is Fc-DNA. A moderate yield of 35% was obtained. Two factors may affect the yield. One is the purity of NH_2-DNA and the second is that the reaction has been carried out under heterogeneous conditions.

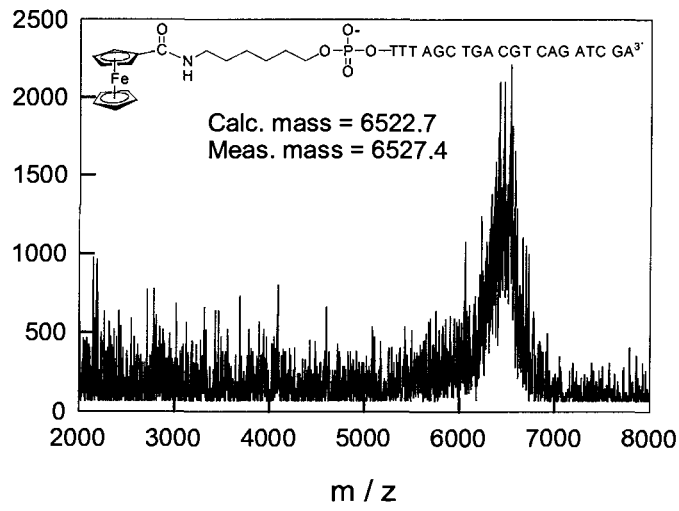

Figure 4-5 MALDI-TOF mass spectrometry of HPLC peak collected at 12.4 min indicating the formation of Fc-DNA.

4.3.2 Electrochemical Study of Fc-DNA-Modified Gold Electrodes

The electrochemical measurements were carried out in 50 mM NaCl / 10 mM Tris-HCl at pH 7.4. A typical voltammogram of Fc-dsDNA (a) is shown in Figure 4.6A. A pair of redox peaks have been observed, with formal potential ($E^{o'}$) of +392 mV (vs. Ag|AgCl) and peak separation (ΔEp) of 16 mV at the scan rate of 0.1 V/s. During

forward potential scan, ferrocene can release an electron to the gold electrode forming the ferrocenium cation that will be reduced back to ferrocene during the backward potential scan. Plotting the anodic peak current against the scan rate shows a linear relationship (Figure 4.6B), showing the presence of surface-bound ferrocene.

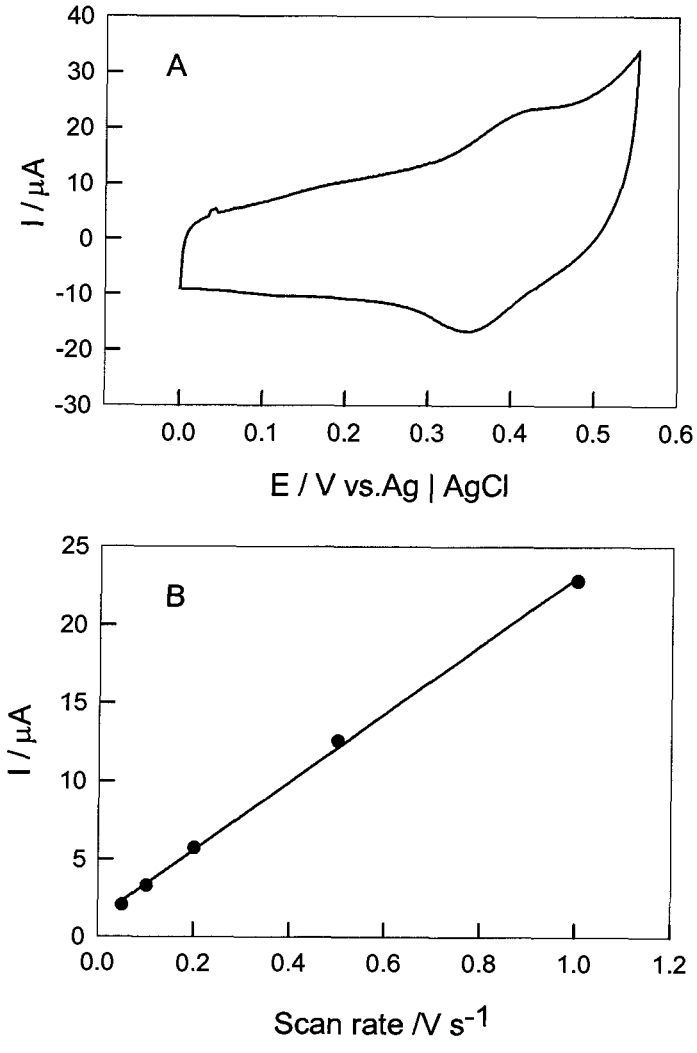

Figure 4-6 **(A) CV of HS-dsDNA-Fc synthesized in our lab in 50 mM NaCl, 10mM Tris-HCl at pH 7.4. The scan rate was 1 V/s. (B) Linear dependence of peak currents on scan rates from 0.05 V/s to 1 V/s.**

Since only one Fc molecule is attached to each DNA helix, the total number of Fc head groups corresponds to the DNA-surface density providing that all the redox labels are electroactive under the conditions of testing. The total amount of surface-bound Fc moieties can be determined quantitatively from the area under the anodic peak, corrected for the background current in the CV, using the following relation:

$$\Gamma_{Fc-DNA} = (\frac{Q}{nFA})N_A \qquad 4.1$$

where Q is the charge obtained by integration of the oxidation peak of surface-bound ferrocene, n is the number of electrons involved in the redox reaction, F is the Faraday constant, A is electrode area and N_A is the Avagadro's number. The surface density calculated by this method is $(1.54 \pm 0.16) \times 10^{12}$ molecules/cm^2.

Furthermore, the surface density can be calculated in an alternate way by treating the same electrode with 3.5 μM $[Ru(NH_3)_6]Cl_3$ solution (as described in Chapters 1 and 2). The surface density of the DNA probes can be determined from the relationship,

$$\Gamma_{Ru-DNA} = (\frac{Q}{nFA})(\frac{Z}{m})N_A \qquad 4.2$$

where Q is the charge obtained by integration of the cathodic peak of $[Ru(NH_3)_6]^{3+}$ in the cyclic voltammogram, n is the number of electrons transferred in the reaction, F is the Faraday Constant, Z is the charge of the redox molecule and m is the number of nucleotides in the DNA. Surface density of DNA calculated by this method is $(3.06 \pm 0.11) \times 10^{12}$ molecules/cm^2

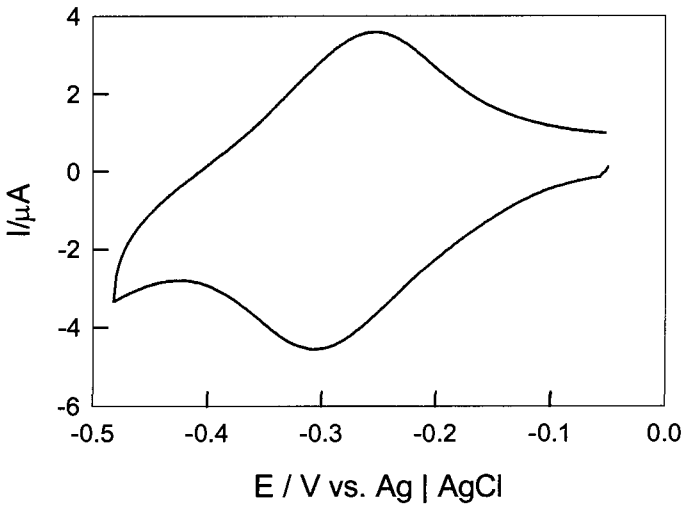

Figure 4-7 Cyclic voltammogram obtained by incubating Fc-dsDNA-modified electrodes in 3.5 μM $[Ru(NH_3)_6]^{3+}$ solution in 10 mM Tris-HCl at pH 7.4. The scan rateused was 50 mV/s.

The values of surface densities obtained from Equations 4.1 and 4.2 are at the same order although they differ from each significantly. The difference may due to the situation when some of the thiolated DNA-strands on the surface are not hybridized with the complimentary ferrocene-terminated complementary strands.

In comparison with the SAMs of ferrocenyl alkanethiols on gold (theoretical surface coverage is 2.5×10^{14} molecules/cm^2, based on a closely packed layer of 0.66 nm diameter spheres[10]), the surface density of Fc-DNA on gold is about two orders of magnitude lower. Attaching multiple ferrocene groups to DNA may be a way to increase the surface density of ferrocene on DNA-modified surfaces and therefore to amplify the electrochemical signal.[11]

4.4 Conclusion

Ferrocene -tethered oligonucleoides have been prepared and used to modify gold electrodes, which showed ideal electrochemical behavior. The surface density of the Fc-dsDNA was calculated and the value of the surface density of the DNA was comparable with the values published in literature.

Successful observation of the redox signal of ferrocene covalently bound to oligonucleotide-modified surfaces is the first step toward developing a DNA/aptamer biosensor for electrochemical detection of analytes, if analyte binding induces a change of the DNA conformation and therefore the charge transfer pathway.

4.5 References

1. (a) Yu, H.-Z.; Luo, C.-Y.; Sankar, C. G.; Sen, D. *Anal. Chem.* **2003,** *75,* 3902-07; (b) Su, L.; Sankar, C. G.; Yu, H.-Z.; Sen, D. *Anal. Chem.* **2004,** *76,* 5953-59; (c) Su, L.; Sen. D.; Yu, H.-Z.; *Analyst* **2006,** *131,* 317-322.
2. Palacek, E.; Jelen, F. *Crit. Rev. Anal. Chem.* **2002,** *32.* 261-70.
3. Armistead, P.M.; Thorp, H.H. *Anal. Chem.* **2000**, *76*, 3764-70.
4. Kelley, S. O.; Boon, E. M.; Barton, J. K.; Jackson, N. M.; Hill, M. G. *Nucleic Acids Res.* **1999**, *27*, 4830-37
5. Boon, E. M.; Ceres, D. M.; Drummond, T. G.; Hill, M. G.; Barton, J. K. *Nat. Biotechnol,* **2000,** *18,* 1096-1100.
6. Long, Y-T.; Li, C. Z.; Sutherland, T. C.; Chahma, M.; Lee, J. S.; Kraatz, H-B. *J. Am. Chem. Soc,* **2003,** *125,* 8724-25.
7. (a) Anne, A.; Bouchardon, A.; Moiroux, J. *J. Am. Chem. Soc.* **2003,** *125,* 1112-13; (b) Anne, A.; Demaille, C. *J. Am. Chem. Soc.* **2006,** *128,* 542-57.
8. Fahlman, R. P.; Sen, D. *J. Am. Chem. Soc,* **2002,** *124,* 4610-16.

9. (a) Takenaka, S.; Uto, Y.: Kondo, H.; Ihara, T.; Takagi, M. *Anal. Biochem.* **1994**, *218*, 436-443; (b) Ihara, T.; Maruo, Y.; Takenaka, S.; Takagi, M. *Nucleic Acids Res.* **1996**, 24, 4273-4280.

10. Viana, A. S.; Jones, A. H.; Abrantes, L. M.; Kalaji, M. *J. Electroanal. Chem.* **2001**, 500, 290-298.

11. Wang, J.; Li, J.; Baca, A. J.; Hu, J.; Zhou, F.; Yan, W.; Pang, D.-W. *Anal.Chem.* **2003**, 75, 3941-3945.

CHAPTER 5
CONCLUDING REMARKS AND FUTURE WORK

In summary, this thesis describes electrochemical studies on and the sensing applications of DNA-modified surfaces, and essentially extends the perspectives of direct electrochemical detection methods in DNA-sensing technology.

The data presented in Chapter 2 demonstrate that a simple voltammetric procedure can be used to study the interaction of aptamer-lysozyme binding. In particular, the electrochemical response of $[Ru(NH_3)_6]^{3+}$ and $[Fe(CN)_6]^{3-}$ on anti-lysozyme aptamer-modified surfaces were studied. From the resulting CVs, it was found that the electrochemical response of $[Ru(NH_3)_6]^{3+}$ decreases, while that of $[Fe(CN)_6]^{3-}$ increases upon binding to lysozyme. The change of the signal is found to be a function of lysozyme concentration. A correlation between the sensor sensitivity and surface density of aptamer was also evident.

Chapter 3 reports our attempt to study ds-DNA-modified surfaces using a redox intercalator, 9,10-Anthraquinone-2,6-disulfonic acid. Chapter 4 describes the synthesis and characterization of a ferrocene-terminated oligonucleotide (Fc-DNA). The electrochemical behavior of the Fc-DNA-modified surface has also been studied.

In the future, other sensing applications based on the electrochemical protocol described in Chapter 2 could be explored, such as detecting single-base mismatches in a DNA duplex using MutS, a protein known to bind only to mismatches. A thiolated DNA probe strand containing a single base mismatch could be immobilized on the gold

surface. Upon exposing the sample to a solution containing $[Ru(NH_3)_6]^{3+}$ at equilibrium, a cyclic voltammetric response from $[Ru(NH_3)_6]^{3+}$ could be obtained. By adding MutS to the electrolyte solution, the voltammetric response should be decreased due to the binding of the protein to the mismatched DNA strand.

Again, using a redox intercalator, as described in Chapter 3, is another option for detecting aptamer-analyte binding. Thiolated probe aptamer sequences can be immobilized on gold electrode surfaces and hybridized with the complementary sequence, followed by incubation with the redox intercalator. Electron transfer through the DNA duplex can be studied by monitoring the electrochemical behavior of the intercalator before and after binding to the analyte.

Based on the synthetic routes developed in Chapter 4, quantitative analysis of analytes, such as adenosine, can be carried out using a ferrocene-attached anti-adenosine aptamer. Thiolated DNA can be hybridized with a ferrocene-attached complementary sequence in solution to form a duplex containing an aptamer sequence and immobilized on a gold electrode surface. In principle, upon incubation with a solution containing the analyte, the redox peaks of the attached ferrocene-moiety should increase due to the regeneration of the base stacking in the duplex. Similarly, quantitative analysis of other analytes is also possible using this method.